VILA DO CONDE,
PORTUGAL,
29-31 MARCH, 2016

11th Iberian Cosmology Meeting

IBERICOS 2016

SERIES OF MEETINGS WHICH AIM TO ENCOURAGE INTERACTIONS AND COLLABORATIONS BETWEEN RESEARCHERS WORKING IN COSMOLOGY AND RELATED AREAS IN PORTUGAL AND SPAIN.

www.iastro.pt/ibericos2016

ia instituto de astrofísica e ciências do espaço

FCT Fundação para a Ciência e a Tecnologia

U.PORTO

Vila do Conde

TEATRO MUNICIPAL VILA DO CONDE

The shape of CMB temperature and polarization peaks on the sphere

AMC, R. Fernández-Cobos, E. Martínez-González and P. Vielva (**arXiv:1512.07412**)

A. Marcos-Caballero

Instituto de Física de Cantabria (IFCA)

March 30, 2016

IberiCos 2016, Vila do Conde, Portugal

A field on the sphere is expanded in terms of the spherical harmonics coefficients:

$$T(\theta,\phi) = \sum_{\ell=0}^{\infty} \sum_{m=-\ell}^{\ell} a_{\ell m}\ Y_{\ell m}(\theta,\phi)$$

Covariant derivatives in the helicity basis $\mathbf{e}_{\pm} = (\mathbf{e}_\theta \pm i\mathbf{e}_\phi)/\sqrt{2}$:

$$\nabla_+ = -\frac{1}{\sqrt{2}}\eth\ , \qquad \nabla_- = -\frac{1}{\sqrt{2}}\eth^*\ .$$

$\eth$ and $\eth^*$ are the spin raising and lowering operators:

$$\eth\,({}_sY_{\ell m}) = \sqrt{\ell(\ell+1) - s(s+1)}\ {}_{s+1}Y_{\ell m}\ ,$$

$$\eth^*\,({}_sY_{\ell m}) = -\sqrt{\ell(\ell+1) - s(s-1)}\ {}_{s-1}Y_{\ell m}\ .$$

First order derivatives

Gradient:

$$\eth T = -\partial_\theta T - i\partial_\phi T$$

$\eth^* T = (\eth T)^*$

Second order derivatives

The Hessian matrix is decomposed into its irreducible parts:

$$\partial_i \partial_j T = \underbrace{\frac{1}{2}\nabla^2 T \delta_{ij}}_{\text{Trace part}} + \underbrace{\left(\partial_i \partial_j - \frac{1}{2}\delta_{ij}\nabla^2\right) T}_{\text{Traceless symmetric part}}$$

Trace: $\nabla^2 T = \eth^* \eth T$.

Traceless symmetric: $\eth^2 T = \partial_\theta^2 T - \partial_\phi^2 T + 2i\partial_\theta \partial_\phi T$ and $\left(\eth^*\right)^2 T = \left(\eth^2 T\right)^*$

The derivatives can be expressed in terms of the spherical harmonics coefficients.

- Scalars ($s = 0$): T and $\nabla^2 T$.
- Vector ($s = 1$): $\eth T$.
- Tensor ($s = 2$): $\eth^2 T$.

When the derivatives are taken at the north pole, the rank of the tensors are classified by the multipole m.

At the north pole:

$$T = \sum_{\ell=0}^{\infty} \sqrt{\frac{2\ell+1}{4\pi}} a_{\ell 0} \ ,$$

$$\eth^* T = \sum_{\ell=0}^{\infty} \sqrt{\frac{2\ell+1}{4\pi}} \sqrt{\frac{(\ell+1)!}{(\ell-1)!}} a_{\ell 1} \ ,$$

$$\nabla^2 T = \eth^* \eth T = -\sum_{\ell=0}^{\infty} \sqrt{\frac{2\ell+1}{4\pi}} \frac{(\ell+1)!}{(\ell-1)!} a_{\ell 0} \ ,$$

$$(\eth^*)^2 T = \sum_{\ell=0}^{\infty} \sqrt{\frac{2\ell+1}{4\pi}} \sqrt{\frac{(\ell+2)!}{(\ell-2)!}} a_{\ell 2} \ .$$

The peak variables

$$\nu \equiv \frac{T}{\sigma_\nu} \ , \qquad \kappa \equiv -\frac{\nabla^2 T}{\sigma_\kappa} \ , \qquad \eta \equiv \frac{\partial^* T}{\sigma_\eta} \ , \qquad \epsilon \equiv \frac{(\partial^*)^2 T}{\sigma_\epsilon} \ .$$

$$\nu = \sum_{\ell=0}^{\infty} \nu_\ell a_{\ell 0} \ , \quad \kappa = \sum_{\ell=0}^{\infty} \kappa_\ell a_{\ell 0} \ , \quad \eta = \sum_{\ell=0}^{\infty} \eta_\ell a_{\ell 1} \ , \quad \epsilon = \sum_{\ell=0}^{\infty} \epsilon_\ell a_{\ell 2} \ .$$

Orthogonalization process...

$$a_{\ell 0} = \hat{a}_{\ell 0} + \begin{pmatrix} \nu_\ell & \kappa_\ell \end{pmatrix} \Sigma^{-1} \left[\begin{pmatrix} \nu \\ \kappa \end{pmatrix} - \sum_{\ell'=0}^{\infty} \begin{pmatrix} \nu_{\ell'} \\ \kappa_{\ell'} \end{pmatrix} \hat{a}_{\ell' 0} \right] \ ,$$

$$a_{\ell 1} = \hat{a}_{\ell 1} + \eta_\ell \left(\eta - \sum_{\ell'=0}^{\infty} \eta_{\ell'} \hat{a}_{\ell' 1} \right) \ ,$$

$$a_{\ell 2} = \hat{a}_{\ell 2} + \epsilon_\ell \left(\epsilon - \sum_{\ell'=0}^{\infty} \epsilon_{\ell'} \hat{a}_{\ell' 2} \right) \ ,$$

$$a_{\ell m} = \hat{a}_{\ell m} \quad (m > 2) \ .$$

$\hat{a}_{\ell m}$ and the peak variables ν, κ, η and ϵ have no correlations.

Variances of the peak degrees of freedom:

$$\sigma_\nu^2 = \sum_{\ell=0}^{\infty} \frac{2\ell+1}{4\pi} C_\ell^{TT} \ ,$$

$$\sigma_\kappa^2 = \sum_{\ell=0}^{\infty} \frac{2\ell+1}{4\pi} \left[\frac{(\ell+1)!}{(\ell-1)!}\right]^2 C_\ell^{TT} \ ,$$

$$\sigma_\eta^2 = \sum_{\ell=1}^{\infty} \frac{2\ell+1}{4\pi} \frac{(\ell+1)!}{(\ell-1)!} C_\ell^{TT} \ ,$$

$$\sigma_\epsilon^2 = \sum_{\ell=2}^{\infty} \frac{2\ell+1}{4\pi} \frac{(\ell+2)!}{(\ell-2)!} C_\ell^{TT} \ .$$

Constraint equation

$$\sigma_\kappa^2 - \sigma_\epsilon^2 = 2\sigma_\eta^2$$

In the sphere, $\sigma_\kappa^2 \neq \sigma_\epsilon^2$

$$a = \sigma_\kappa^2 / \sigma_\epsilon^2$$

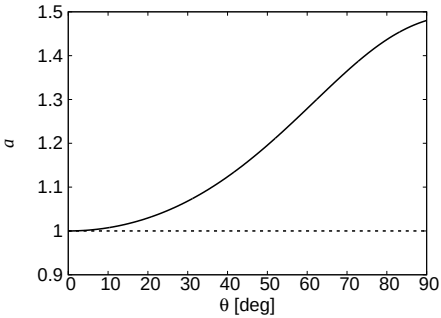

Flat approx. $a \to 1$.

Probability density of the peak variables:

$$P(\nu,\kappa,\epsilon)\,\mathrm{d}\nu\,\mathrm{d}\kappa\,\mathrm{d}^2\epsilon = \frac{2|\epsilon|}{2\pi\sqrt{(1-\rho^2)}}\exp\left[-\frac{\nu^2-2\rho\nu\kappa+\kappa^2}{2(1-\rho^2)}-|\epsilon|^2\right]\,\mathrm{d}\nu\,\mathrm{d}\kappa\,\mathrm{d}|\epsilon|\,\frac{\mathrm{d}\alpha}{\pi}\,.$$

Peak constraints:

- Constraints over the peak height: $\nu=\nu_0$ or $\nu>\nu_t$
- Critical point: $\eta=0$,
- Extremum: $|\epsilon|\leq\sqrt{a}|\kappa|$,

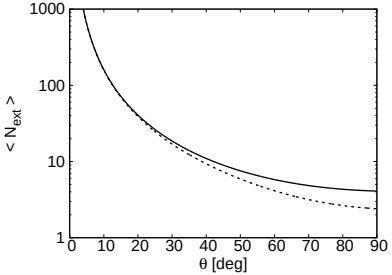

Number density of critial points:

$$n(\nu,\kappa,\epsilon)\,\mathrm{d}\nu\,\mathrm{d}\kappa\,\mathrm{d}^2\epsilon = \frac{1}{2\pi\theta_*^2}\left(a\kappa^2-|\epsilon|^2\right)P(\nu,\kappa,\epsilon)\,\mathrm{d}\nu\,\mathrm{d}\kappa\,\mathrm{d}^2\epsilon\,,$$

$$\langle N_{\rm ext}\rangle = 2\left(1+\frac{1}{\theta_*^2\sqrt{3+2\theta_*^2}}\right).$$

where $a=1+\theta_*^2$.

Multipolar profiles

Given the polar coordinates around a peak, the multipolar profile $X_m(\theta)$ is the Fourier transform of the azimuthal angle as a function of θ:

$$X(\theta,\phi) = \sum_{m=-\infty}^{\infty} X_m(\theta)\ e^{im\phi}\ .$$

Inverse transform:

$$X_m(\theta) = \frac{1}{2\pi}\int \mathrm{d}\phi\ X(\theta,\phi)\ e^{-im\phi}\ .$$

The multipolar profiles can be expanded in terms of the associated Legendre polynomial $P_\ell^m(\cos\theta)$:

$$X_m(\theta) = \sum_{\ell=m}^{\infty}\sqrt{\frac{2\ell+1}{4\pi}}\sqrt{\frac{(\ell-m)!}{(\ell+m)!}}\ a_{\ell m}^X\ P_\ell^m(\cos\theta)\ .$$

$$\langle T_0(\theta)\rangle = \sum_{\ell=0}^{\infty} \frac{2\ell+1}{4\pi}\left[b_\nu + b_\kappa \ell(\ell+1)\right] C_\ell^{TT}\ P_\ell(\cos\theta)\ ,$$

$$\langle Q_{r0}(\theta)\rangle = -\sum_{\ell=2}^{\infty} \frac{2\ell+1}{4\pi}\sqrt{\frac{(\ell-2)!}{(\ell+2)!}}\left[b_\nu + b_\kappa \ell(\ell+1)\right] C_\ell^{TE}\ P_\ell^2(\cos\theta)\ ,$$

$$\langle U_{r0}(\theta)\rangle = -\sum_{\ell=2}^{\infty} \frac{2\ell+1}{4\pi}\sqrt{\frac{(\ell-2)!}{(\ell+2)!}}\left[b_\nu + b_\kappa \ell(\ell+1)\right] C_\ell^{TB}\ P_\ell^2(\cos\theta)\ .$$

$$\langle T_2(\theta)\rangle = b_\epsilon \sum_{\ell=0}^{\infty} \frac{2\ell+1}{4\pi} C_\ell^{TT}\ P_\ell^2(\cos\theta)\ ,$$

$$\langle Q_{r2}(\theta)\rangle = -2b_\epsilon \sum_{\ell=0}^{\infty} \frac{2\ell+1}{4\pi}\sqrt{\frac{(\ell-2)!}{(\ell+2)!}}\left[C_\ell^{TE}\ P_\ell^+(\cos\theta) + iC_\ell^{TB}\ P_\ell^-(\cos\theta)\right]\ ,$$

$$\langle U_{r2}(\theta)\rangle = 2ib_\epsilon \sum_{\ell=0}^{\infty} \frac{2\ell+1}{4\pi}\sqrt{\frac{(\ell-2)!}{(\ell+2)!}}\left[C_\ell^{TE}\ P_\ell^-(\cos\theta) + iC_\ell^{TB}\ P_\ell^+(\cos\theta)\right]\ .$$

Biases

$$\begin{pmatrix} b_\nu\sigma_\nu \\ b_\kappa\sigma_\kappa \end{pmatrix} = \Sigma^{-1}\begin{pmatrix} \langle\nu\rangle \\ \langle\kappa\rangle \end{pmatrix}\ ,$$

$$b_\epsilon = \frac{\langle\epsilon\rangle}{\sigma_\epsilon}\ .$$

non-local anisotropic bias:

$$X(\theta) = b\ \mathbf{C}^{TX}(\theta)$$

$$b = b_\nu - (b_\kappa - 2|b_\epsilon|)\,\partial_x^2 - (b_\kappa + 2|b_\epsilon|)\,\partial_y^2$$

T Q_r U_r

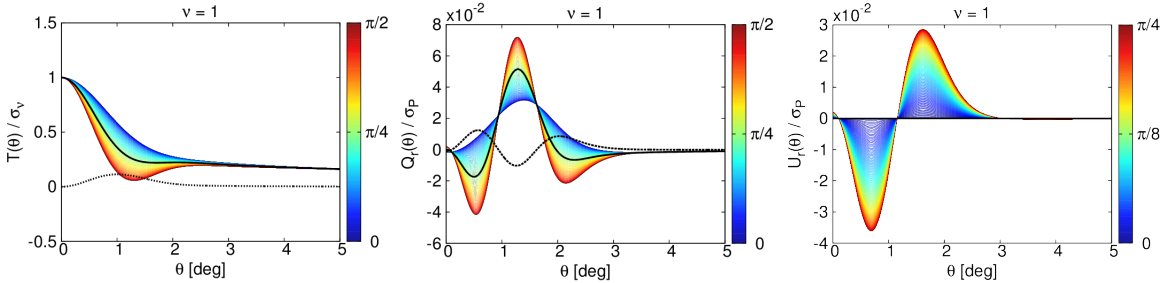

- The effect of the eccentricity modify the profile up to the sound horizon scale.
- The acoustic oscillations in the polarization field are modulated between the principal directions.

- The pressure of the photon fluid in the minor axis of the peak is higher than in the major one. This implies a quadrupole aligned with the principal axes in Q_r.
- The flow of photons is not radial for elliptical peaks, which introduces a non-zero U_r. This effect is particularly dominant at 45°, whose pattern forms a quadrupole at 45° with respect to the principal axes.

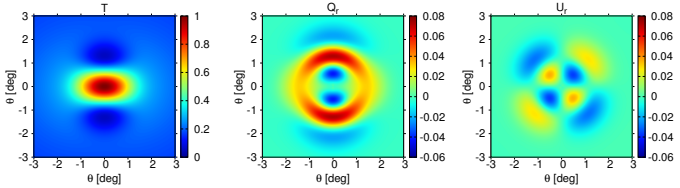

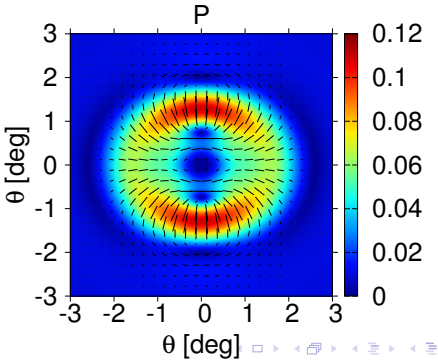

Summary and conclusions

- A theoretical study of CMB temperature peaks, including its effect over the polarization field, and allowing nonzero eccentricity, is presented.
- Some differences of the peak statistics between the flat space and the sphere are found.
- The covariance matrix of the multipolar profiles and the peak patterns in temperature and polarization are calculated within this formalism.
- The analysis in terms of the spherical harmonics coefficients allows to simulate constrained realizations of the CMB with a given peak present at some position.

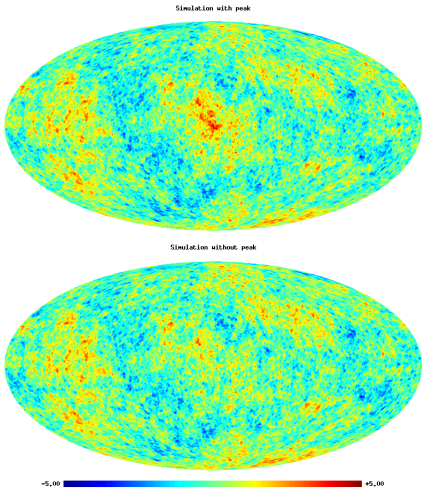

VILA DO CONDE,
PORTUGAL,
29-31 MARCH, 2016

11th Iberian Cosmology Meeting

IBERICOS 2016

SERIES OF MEETINGS WHICH AIM TO ENCOURAGE INTERACTIONS AND COLLABORATIONS BETWEEN RESEARCHERS WORKING IN COSMOLOGY AND RELATED AREAS IN PORTUGAL AND SPAIN.

www.iastro.pt/ibericos2016

ia instituto de astrofísica e ciências do espaço

FCT Fundação para a Ciência e a Tecnologia

U.PORTO

Vila do Conde

TEATRO MUNICIPAL VILA DO CONDE

Exploring 2-spin internal linear combinations for the recovery of the CMB polarization

Raúl Fernández-Cobos, Airam Marcos-Caballero, Patricio Vielva, Enrique Martínez-González, R. Belén Barreiro

Instituto de Física de Cantabria

March 30^{th}, 2016

Recovery of the CMB component

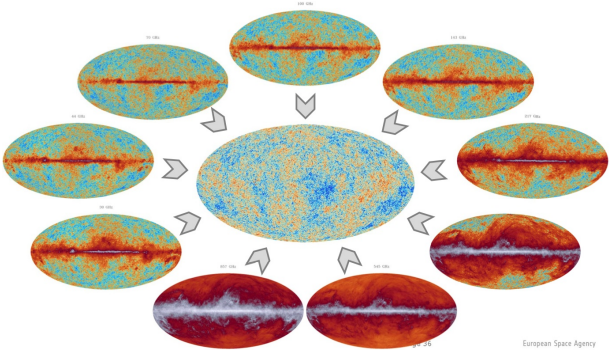

Internal linear combination (ILC):

$$\hat{T}_{\rm CMB} = \sum_{j=1}^{N_\nu} \omega_j T_i, \quad \text{with} \sum_{j=1}^{N_\nu} \omega_j = 1.$$

- Blind approach: it only assumes that the CMB is constant in the frequency range (black body spectrum). $T_i \equiv T_{\rm CMB} + F_i$
- The ω_j coefficients are computed by minimizing $\left\langle T^2 \right\rangle - \left\langle T \right\rangle^2$.

A description of the CMB polarization

Stokes parameters

$$I = |E_1|^2 + |E_2|^2 \quad Q = \frac{1}{4}\left(|E_1|^2 - |E_2|^2\right)$$
$$U = \frac{1}{2}\mathrm{Re}\left(E_1^* E_2\right) \quad V = \frac{1}{2}\mathrm{Im}\left(E_1^* E_2\right)$$

In the helicity basis $\epsilon^{\pm} = \left(\epsilon^{(1)} + i\epsilon^{(2)}\right)/\sqrt{2}$:

- I is the intensity of the electromagnetic wave.
- V is the difference between left- and right-handed circular polarization (expected to be null on the CMB).
- $Q \pm iU$ are 2-spin quantities with magnetic quantum number ± 2, and describe the linear polarization.

$$\begin{aligned}
\mathbf{P}_{ij} &= \tilde{\mathcal{P}}_{ab}\epsilon_i^{(a)}\epsilon_j^{(b)} \\
\tilde{\mathcal{P}}_{ab} &= E_a^* E_b \\
&= \frac{1}{2}\left[I\sigma_{ab}^{(0)} + U\sigma_{ab}^{(1)} + V\sigma_{ab}^{(2)} + Q\sigma_{ab}^{(3)}\right]
\end{aligned}$$

$$\sigma^{(0)} = \begin{pmatrix} 1 & 0 \\ 0 & 1 \end{pmatrix}, \quad \sigma^{(1)} = \begin{pmatrix} 0 & 1 \\ 1 & 0 \end{pmatrix}, \quad \sigma^{(2)} = \begin{pmatrix} 0 & -i \\ -i & 0 \end{pmatrix}, \quad \sigma^{(3)} = \begin{pmatrix} 1 & 0 \\ 0 & -1 \end{pmatrix}$$

ILC polarization implementation

- PILC solution (arXiv:1601.01515): recovery of the CMB polarization $\hat{Q}_{\rm CMB}$ and $\hat{U}_{\rm CMB}$:

$$\hat{Q}_{\rm CMB}(p) \pm i\hat{U}_{\rm CMB}(p) = \sum_{j=1}^{N_\nu} \left[\omega_j^{(R)} \pm i\omega_j^{(I)}\right] [Q_j(p) \pm iU_j(p)]$$

- Constraints:

$$\begin{aligned} \sum_{j=1}^{N_\nu} \omega_j^{(R)} &= 1 \\ \sum_{j=1}^{N_\nu} \omega_j^{(I)} &= 0 \end{aligned}$$

ILC polarization implementation

- The $\omega_j^{(R)}$ and $\omega_j^{(I)}$ coefficients are computed by minimizing:

$$\begin{aligned}\left\langle P^2_{\rm CMB}\right\rangle &= \left\langle \left[\hat{Q}_{\rm CMB}(p) + i\hat{U}_{\rm CMB}(p)\right]\left[\hat{Q}_{\rm CMB}(p) - i\hat{U}_{\rm CMB}(p)\right]\right\rangle \\ &= \begin{pmatrix} \left[\boldsymbol{\omega}^{(R)}\right]^T & \left[\boldsymbol{\omega}^{(I)}\right]^T \end{pmatrix} \begin{pmatrix} \mathbf{C}^{(+)} & -\mathbf{C}^{(-)} \\ \mathbf{C}^{(-)} & \mathbf{C}^{(+)} \end{pmatrix} \begin{pmatrix} \boldsymbol{\omega}^{(R)} \\ \boldsymbol{\omega}^{(I)} \end{pmatrix}\end{aligned}$$

- Using the method of Lagrange multipliers:

$$\begin{pmatrix} 2\mathbf{C}^{(+)} & -2\mathbf{C}^{(-)} & -\mathbf{1} & \mathbf{0} \\ 2\mathbf{C}^{(-)} & 2\mathbf{C}^{(+)} & \mathbf{0} & -\mathbf{1} \\ \mathbf{1}^T & \mathbf{0}^T & 0 & 0 \\ \mathbf{0}^T & \mathbf{1}^T & 0 & 0 \end{pmatrix} \begin{pmatrix} \boldsymbol{\omega}^{(R)} \\ \boldsymbol{\omega}^{(I)} \\ \lambda_R \\ \lambda_I \end{pmatrix} = \begin{pmatrix} \mathbf{0} \\ \mathbf{0} \\ 1 \\ 0 \end{pmatrix}$$

ILC polarization implementation

- Analytical solution for the coefficients:

$$\begin{aligned}\omega_k^{(R)} &= \frac{\lambda_R}{2}\sum_{l=1}^{N_\nu} C_{kl}^{-1} + \frac{\lambda_I}{2}\sum_{l=N_\nu+1}^{2N_\nu} C_{kl}^{-1},\\ \omega_k^{(I)} &= \frac{\lambda_R}{2}\sum_{l=1}^{N_\nu} C_{N_\nu+k,l}^{-1} + \frac{\lambda_I}{2}\sum_{l=N_\nu+1}^{2N_\nu} C_{N_\nu+k,l}^{-1}\end{aligned}$$

where

$$\mathbf{C} \equiv \begin{pmatrix} \mathbf{C}^{(+)} & -\mathbf{C}^{(-)} \\ \mathbf{C}^{(-)} & \mathbf{C}^{(+)} \end{pmatrix}, \qquad \frac{\lambda_R}{2} = \frac{S_+}{S_+^2 - S_-^2}, \qquad \frac{\lambda_I}{2} = \frac{-S_-}{S_+^2 - S_-^2}$$

and

$$\begin{aligned}C_{kl}^{(+)} &\equiv \langle Q_k(p)Q_l(p) + U_k(p)U_l(p)\rangle\,,\\ C_{kl}^{(-)} &\equiv \langle Q_k(p)U_l(p) - U_k(p)Q_l(p)\rangle\,,\end{aligned}$$

$$S_+ \equiv \sum_{i,j=1}^{N_\nu} C_{ij}^{-1}, \quad S_- \equiv \sum_{i=1}^{N_\nu}\sum_{j=N_\nu+1}^{2N_\nu} C_{ij}^{-1}$$

- $Q \pm iU$ can be expanded in terms of the spin-weighted spherical harmonics ${}_{\pm s}Y_{\ell m}$ as:

$$(Q \pm iU)(\mathbf{n}) = \sum_{\ell=2}^{\infty} \sum_{m=-\ell}^{\ell} a_{\ell m}^{\pm 2} \, {}_{\pm 2}Y_{\ell m}(\mathbf{n})$$

  with $a_{\ell m}^{\pm 2} = e_{\ell m} \pm i b_{\ell m}$.

- In terms of the E- and B-mode spherical harmonics, the PILC method is seen as:

$$\begin{pmatrix} \hat{e}_{\ell m}^{(\mathrm{CMB})} \\ \hat{b}_{\ell m}^{(\mathrm{CMB})} \end{pmatrix} = \sum_{j=1}^{N_\nu} \begin{pmatrix} \omega_j^{(R)} & -\omega_j^{(I)} \\ \omega_j^{(I)} & \omega_j^{(R)} \end{pmatrix} \begin{pmatrix} e_{\ell m}^j \\ b_{\ell m}^j \end{pmatrix}$$

Comparison with other approaches

- QUILC: applying the scalar ILC method directly to Q and U.
  - $\hat{Q}_{\rm CMB} = \sum_{j=1}^{N_\nu} \omega_j^{(Q)} Q_i$, and $\hat{U}_{\rm CMB} = \sum_{j=1}^{N_\nu} \omega_j^{(U)} U_i$.
  - $\sum_{j=1}^{N_\nu} \left[\omega_j^{(Q)} Q_j + i\omega_j^{(U)} U_j\right]$ is not a 2-spin quantity $\Rightarrow$ Not covariant methodology.
- Applying the scalar ILC method directly to E and B modes.

$$\begin{pmatrix} \hat{e}_{\ell m}^{(\rm CMB)} \\ \hat{b}_{\ell m}^{(\rm CMB)} \end{pmatrix} = \sum_{j=1}^{N_\nu} \begin{pmatrix} \omega_j^{(E)} & 0 \\ 0 & \omega_j^{(B)} \end{pmatrix} \begin{pmatrix} e_{\ell m}^{j} \\ b_{\ell m}^{j} \end{pmatrix}$$

  - Covariant method, but introduces a non-orientation preserving term:

$$\hat{Q}_{\rm CMB} + i\hat{U}_{\rm CMB} = \sum_{j=1}^{N_\nu} \left[\mu_j^{(EB)} + \eta_j^{(EB)} \mathcal{P}\right] (Q_j + iU_j), \text{ with } \mu_j^{(EB)} \equiv \left[\omega_j^{(E)} + \omega_j^{(B)}\right]/2$$

and $\eta_j^{(EB)} \equiv \left[\omega_j^{(E)} - \omega_j^{(B)}\right]/2$, and $\mathcal{P}$ a parity transformation in the tangent plane.

Comparison with other approaches

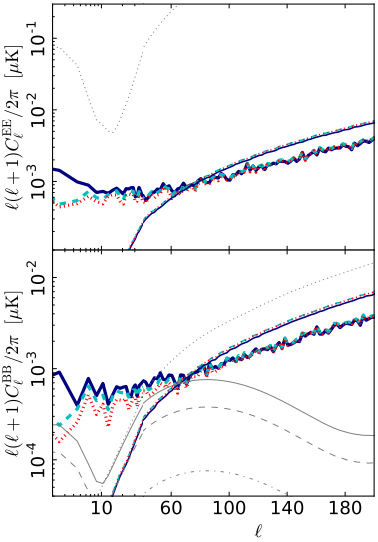

- Angular power spectrum of the residual map from QUILC (navy blue), PILC (cyan) and PRILC (red).
- Differences at low multipoles due to the cross correlation term between CMB and foreground realizations.

Frequency-dependent phase shift

- Complex coefficients induce a frequency-dependent phase shift:

$$\begin{pmatrix} \omega_j^{(R)} & -\omega_j^{(I)} \\ \omega_j^{(I)} & \omega_j^{(R)} \end{pmatrix} = |\omega_j| \begin{pmatrix} \cos(2\phi_j) & -\sin(2\phi_j) \\ \sin(2\phi_j) & \cos(2\phi_j) \end{pmatrix}$$

- The presence of this shift depends only on a non-null combination of channels: $\langle Q_i(p)U_j(p) - U_i(p)Q_j(p)\rangle$, for a pair of frequencies ν_i and ν_j.

Toy model of polarization rotation

- Sets of multi-frequency CMB simulations with a rotated foreground component according the frequency dependence of the Faraday rotation:

$$\phi(\nu) = R_{45} \left(\frac{45\ [\mathrm{GHz}]}{\nu} \right)^2\ [\mathrm{deg}]$$

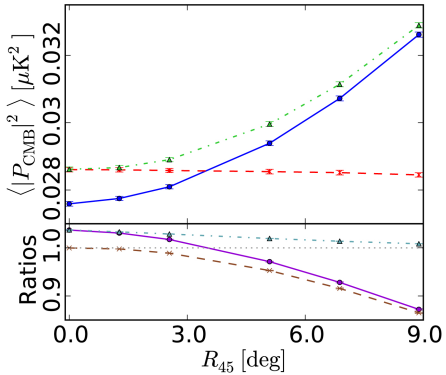

Mean values of the variance of $P_{\mathrm{CMB}} = Q_{\mathrm{CMB}} + iU_{\mathrm{CMB}}$.

- QUILC: blue.
- PILC: red.
- PRILC: green.

Conclusions

- We propose a polarization application of the ILC which takes into account only covariant terms in the coefficient estimation. It preserves the physical properties of the residuals.
- No important differences are found in terms of the pseudo power spectrum of the cleaned simulations with respect to the other implementations.
- The methodology has the potential to be useful in regions in which there is a frequency-dependent shift of the polarization angle such that induced, for instance, by the Faraday rotation.
- In addition, it could be used for estimate the CMB component in alternative scenarios in which the polarization angle changes with frequency, such as some models of birefringence.

VILA DO CONDE,
PORTUGAL,
29-31 MARCH, 2016

11th Iberian Cosmology Meeting

IBERICOS 2016

SERIES OF MEETINGS WHICH AIM TO ENCOURAGE INTERACTIONS AND COLLABORATIONS BETWEEN RESEARCHERS WORKING IN COSMOLOGY AND RELATED AREAS IN PORTUGAL AND SPAIN.

www.iastro.pt/ibericos2016

ia instituto de astrofísica e ciências do espaço

FCT Fundação para a Ciência e a Tecnologia

U.PORTO

Vila do Conde

TEATRO MUNICIPAL VILA DO CONDE

THE DECAY OF THE STANDARD MODEL HIGGS FIELD AFTER INFLATION

Francisco Torrentí, IFT UAM/CSIC

with Daniel G. Figueroa and Juan García-Bellido

11th Iberian Cosmology Meeting, Vila do Conde, 30th March 2016

THE SM HIGGS FIELD DURING/TOWARDS THE END OF INFLATION

Assumption: SM Higgs decoupled from inflationary sector. Inflation is caused by something else which we do not model.

$\xi R\phi^2 = 0$

If ξ < 1/6 ***(massless)*** → **Quantum fluctuations in dS space**

$$\langle\varphi^2\rangle \approx 0.13\frac{H_*^2}{\sqrt{\lambda}} \qquad l_* \gg H_*^{-1} \quad (\lambda(\varphi_*) > 0)$$

If ξ > 1/6 ***(massive)*** → **Sudden drop in R during dS-power law transition**

Herranen *et al* (2015)

$$\langle\varphi^2\rangle \lesssim \mathcal{O}(0.1)\frac{H_*^2}{\lambda\sqrt{\xi}} \qquad l_* \lesssim H_*^{-1}$$

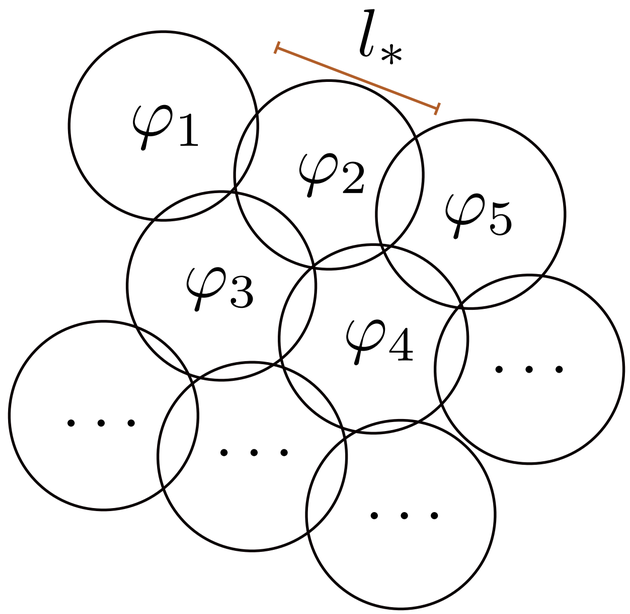

THE SM HIGGS IS EXCITED AFTER THE END OF INFLATION

THE SM HIGGS FIELD AFTER INFLATION

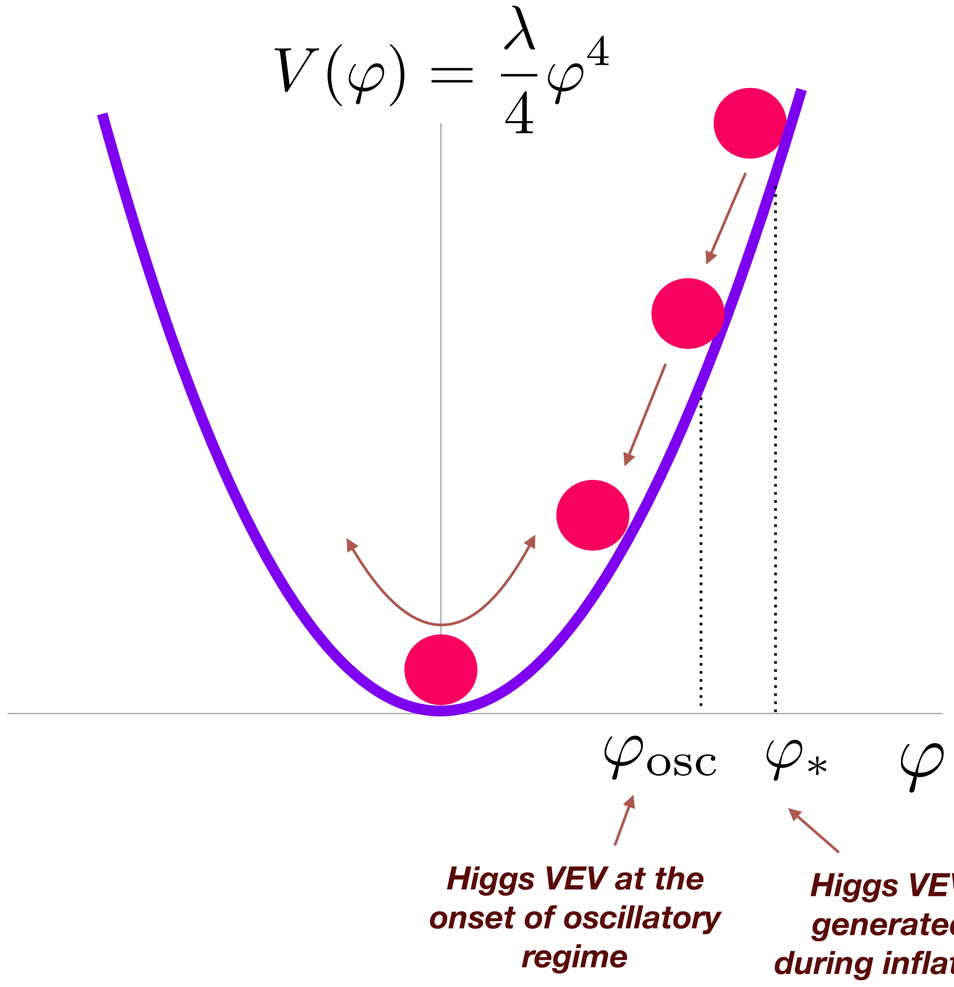

1. **After inflation, the Higgs is frozen in a slow-roll regime.**

2. **Short after inflation ends, the Higgs condensate starts oscillating around the minimum of its potential everywhere in the Universe.**

$$3\lambda\varphi_{\rm osc}^2 \approx H(t_{\rm osc})$$

3. **Every time the Higgs goes through the minimum, all fields coupled directly to it are created.**

$$\frac{1}{\omega_f^2}\frac{d\omega_f}{dt} \gg 1$$

$$\omega_f(t) = \sqrt{k^2 + a^2(t)m_f^2(t)}$$

THE HIGGS DECAYS non-perturbatively:

(particle production in the presence of rapidly changing background fields)

THE SM HIGGS DECAY PRODUCTS

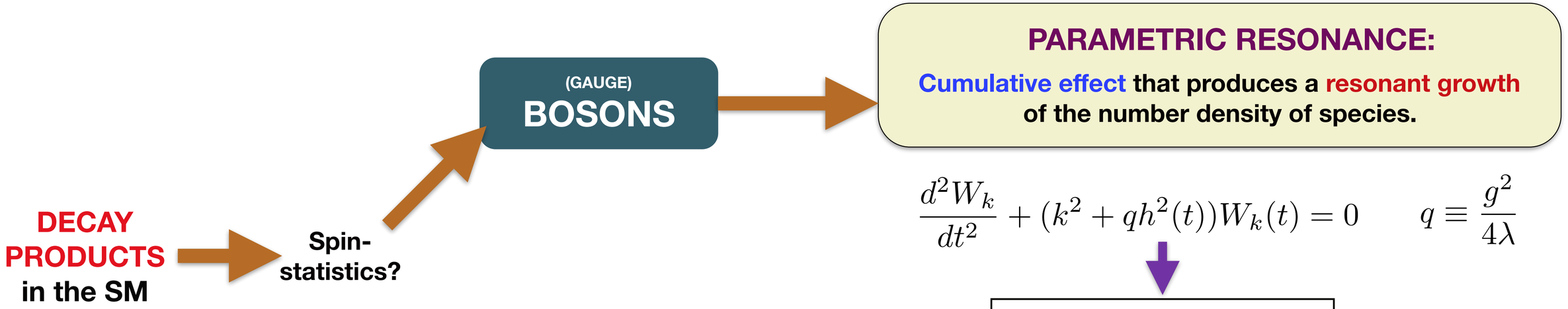

THE SM HIGGS DECAY PRODUCTS

DECAY PRODUCTS in the SM

Spin-statistics?

(GAUGE) BOSONS

PARAMETRIC RESONANCE:

Cumulative effect that produces a resonant growth of the number density of species.

$$\frac{d^2 W_k}{dt^2} + (k^2 + q h^2(t)) W_k(t) = 0 \qquad q \equiv \frac{g^2}{4\lambda}$$

$$n_k \propto |V_k|^2 \propto e^{2\mu_k z}$$

Greene et al. (1997)

PARTICLE CREATION!

FERMIONS

PAULI BLOCKING

$$n_k < 1$$

Energy is transferred to modes of higher momenta in each particle creation burst.

ENERGY TRANSFER MORE EFFICIENT FOR BOSONS THAN FOR FERMIONS

LATTICE SIMULATIONS OF THE SM HIGGS DECAY

- **We solve the Higgs-gauge *eom* in lattice boxes of different sizes ($N^3=(128)^3$ and $N^3=(256)^3$ points). We do not include fermions.**

- **Terms coming from Non-Abelian structure in Lagrangian are at first negligible.**

Abelian-Higgs modelling

- **Simulations correspond to a single patch, inside which we take the initial value of the Higgs φ_* constant.**

RESULTS FROM LATTICE SIMULATIONS

FIRST TIME SCALE: BACKREACTION TIME

Figueroa, García-Bellido & F.T. (2015)

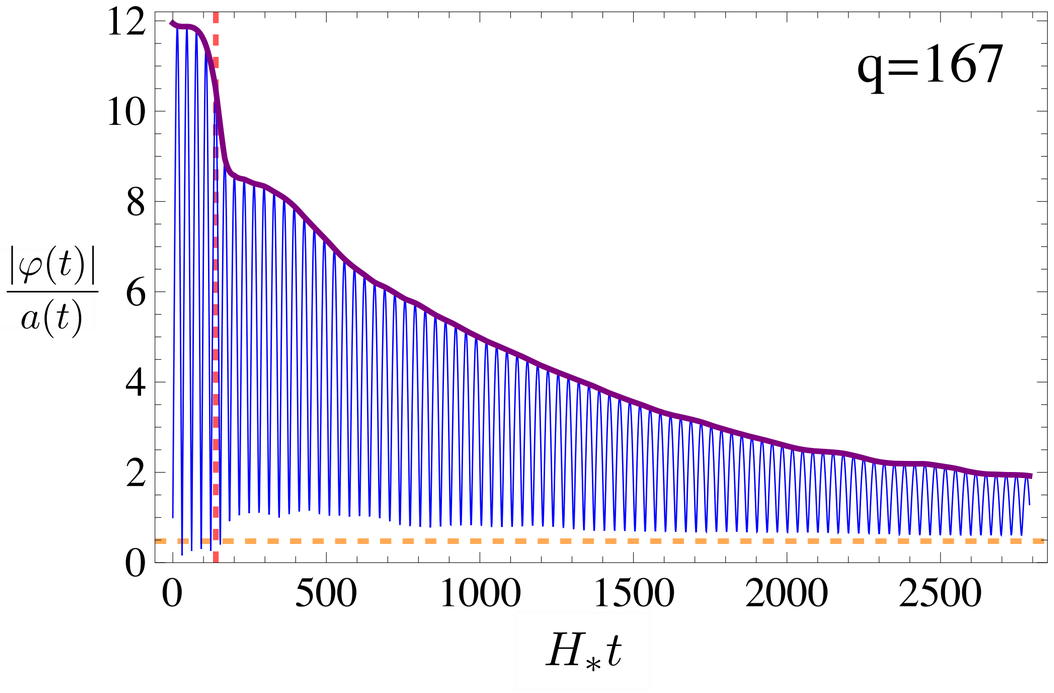

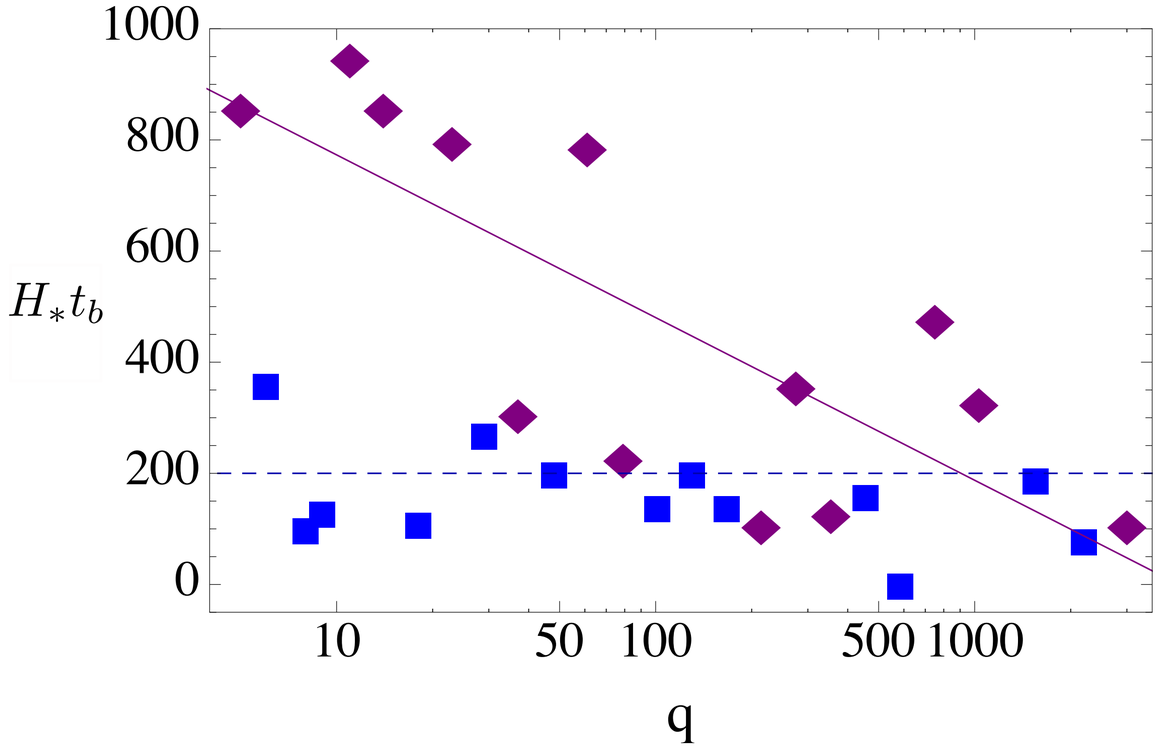

INDICATES WHEN BACKREACTION EFFECTS FROM GAUGE BOSONS ONTO HIGGS CONDENSATE INDUCE THE ONSET OF THE HIGGS DECAY

RESULTS FROM LATTICE SIMULATIONS

SECOND TIME SCALE: DECAY TIME

Figueroa, García-Bellido & F.T. (2015)

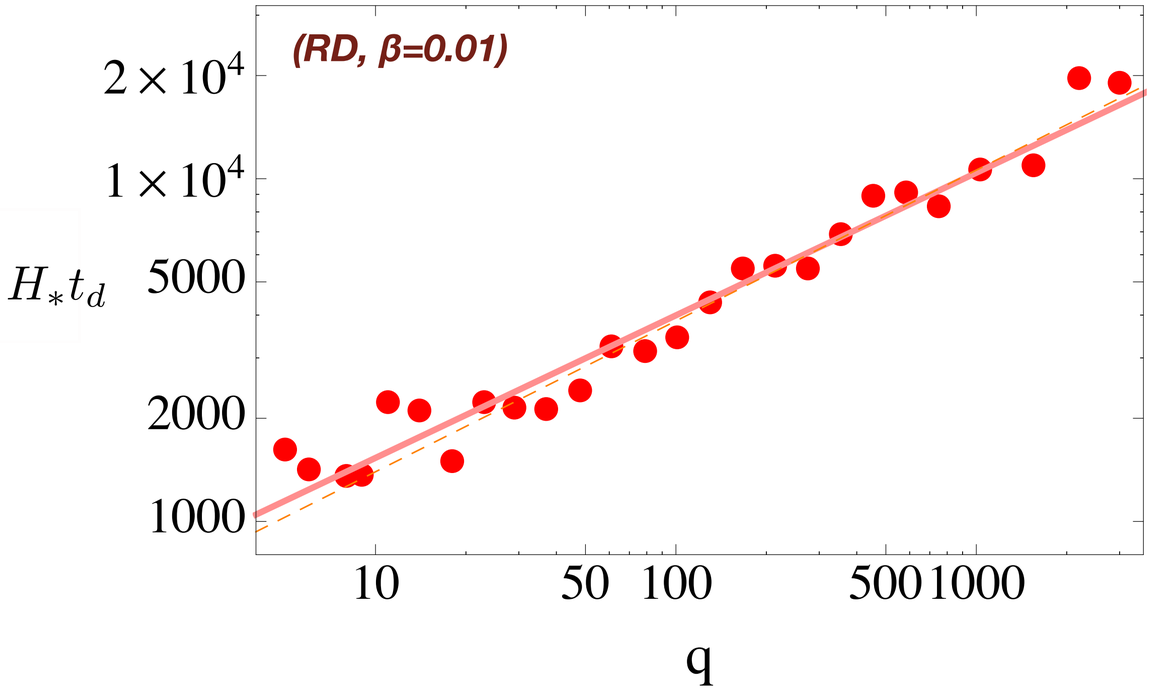

$$t_d \approx 32.8 \left(\frac{\sqrt{\lambda}\varphi_*}{H_*}\right)^{\frac{-(1+3w)}{3(1+w)}} \left(\frac{g_Z^2 + 2g_W^2}{\lambda}\right)^{0.42} H_*^{-1}$$

w **=0,1/3,1 for MD, RD, KD expansion rates**
g_Z, g_W **= Couplings of Higgs to the gauge b.**

INDICATES WHEN THE DECAY OF THE HIGGS HAS FINISHED: A STATIONARY/EQUIPARTITION REGIME HAS BEEN ACHIEVED

GRAVITATIONAL WAVES FROM THE SM HIGGS DECAY

$$\ddot{h}_{ij} + 3H\dot{h}_{ij} - \nabla^2 h_{ij} = \frac{2}{m_p^2}\,\Pi_{ij}^{\mathrm{TT}}$$

$$\Pi_{ij}^{\mathrm{TT}} = \left\{ 2\mathfrak{Re}[(D_i\varphi)^*(D_j\varphi)] + \frac{4}{g^2 a^2(t)} F_i{}^{\alpha} F_{j\alpha} \right\}$$

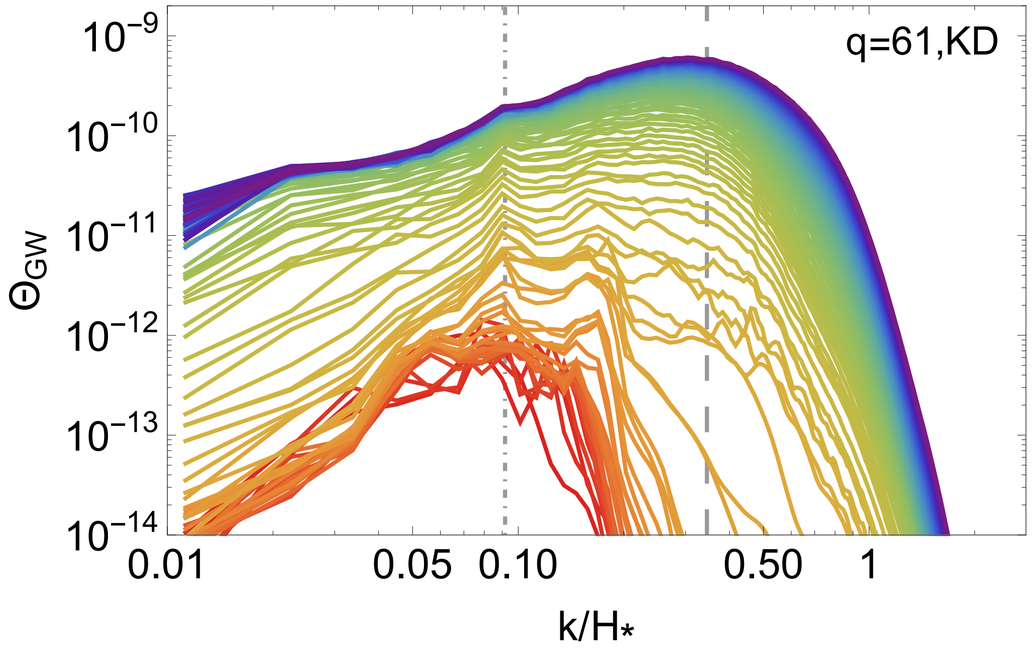

Figueroa, García-Bellido & F.T. (2016)

If we consider standard post-inflationary scenarios, the GW produced are negligible:

RD: $h^2\Omega_{\mathrm{GW}}^{(0)} \lesssim 10^{-29} \qquad f_p \leq 3\cdot 10^8 \mathrm{Hz}$

GRAVITATIONAL WAVES FROM THE SM HIGGS DECAY

$$\ddot{h}_{ij} + 3H\dot{h}_{ij} - \nabla^2 h_{ij} = \frac{2}{m_p^2}\,\Pi_{ij}^{\mathrm{TT}}$$

$$\Pi_{ij}^{\mathrm{TT}} = \left\{ 2\mathfrak{Re}[(D_i\varphi)^*(D_j\varphi)] + \frac{4}{g^2 a^2(t)} F_i{}^{\alpha} F_{j\alpha} \right\}$$

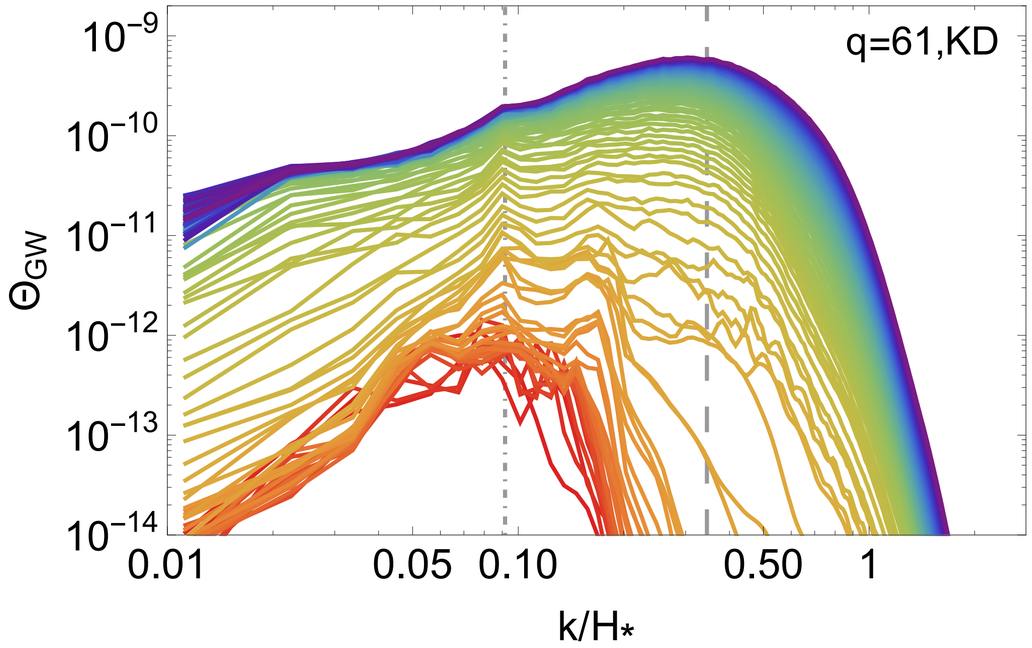

Figueroa, García-Bellido & F.T. (2016)

If we consider standard post-inflationary scenarios, the GW produced are negligible:

RD: $h^2\Omega_{\mathrm{GW}}^{(0)} \lesssim 10^{-29} \qquad f_p \leq 3\cdot 10^{8}\mathrm{Hz}$

The amplitude is enhanced in a Kination-Domination regime after inflation (but very high-frequencies):

KD: $h^2\Omega_{\mathrm{GW}}^{(0)} \lesssim 10^{-16} \qquad f_p \leq 3\cdot 10^{11}\mathrm{Hz}$

CONCLUSIONS

- **We have studied the post-inflationary Higgs decay process with lattice simulations, and parametrized the Higgs dynamics.**

- **As long as the SM Higgs is decoupled form the inflationary sector, the Higgs decay process and its associated GW background is always expected.**

- **However, GW amplitude is negligible and peaked at high frequencies**

just a curiosity of the SM

- **GW signal is enhanced for post-inflationary *kination-domination* regimes, such as Higgs-Reheating** Figueroa & Byrnes (to be published)

VILA DO CONDE,
PORTUGAL,
29-31 MARCH, 2016

11th Iberian Cosmology Meeting

IBERICOS 2016

SERIES OF MEETINGS WHICH AIM TO ENCOURAGE INTERACTIONS AND COLLABORATIONS BETWEEN RESEARCHERS WORKING IN COSMOLOGY AND RELATED AREAS IN PORTUGAL AND SPAIN.

www.iastro.pt/ibericos2016

ia instituto de astrofísica e ciências do espaço

FCT Fundação para a Ciência e a Tecnologia

U.PORTO

Vila do Conde

TEATRO MUNICIPAL VILA DO CONDE

Medium effects in dark matter scattering

Introduction

GR boosted velocity

Cross-Section

Dark matter particle-nucleon interaction

Differential cross-section per unit volume

Cross-section and mean free path

Conclusions

Medium effects in dark matter scattering

M. Cermeño[1], M. A. Pérez-García[1], J. Silk[2]

[1] University of Salamanca, Spain
[2] Institute d'Astrophysique, París, France

March 30, 2016

Introduction

Medium effects in dark matter scattering
Introduction
GR boosted velocity
Cross-Section
Dark matter particle-nucleon interaction
Differential cross-section per unit volume
Cross-section and mean free path
Conclusions

- Interaction: fermionic dark matter particle χ and nucleon N in the neutron star core.
- In previous works (Spergel, D. N. and Press, W. H. 1985, ApJ, 294, 663) in the Sun the DM mean free path has been estimated as $\lambda_\chi \simeq \frac{1}{\sigma_{\chi N} n} \simeq 29.41\ 10^8$ m, where $n = 8.5\ 10^{-16}\ \mathrm{fm}^{-3}$ the ordinary particle number density.
- We calculate the DM mean free path λ_χ inside a neutron star taking into account:

  Temperature, $T \lesssim 50$ MeV
  Density: Pauli blocking, $n \lesssim 2 n_{sat}$,
  $n_{sat} = 0.17\ \mathrm{fm}^{-3}$

  For $R_{NS} = 12$ km and $M_{NS} = 1.5 M_\odot$

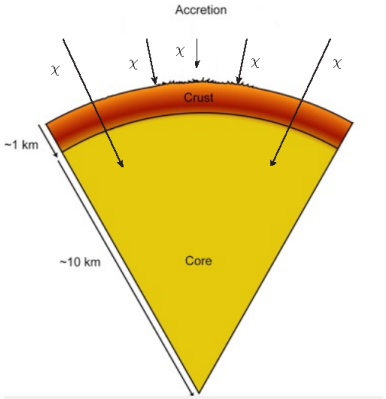

GR boosted velocity

Medium effects in dark matter scattering
Introduction
GR boosted velocity
Cross-Section
Dark matter particle-nucleon interaction
Differential cross-section per unit volume
Cross-section and mean free path
Conclusions

- Schwarzschild metric:

$$ds^2 = -\left(1 - \frac{2GM_{NS}}{c^2 r}\right) c^2 dt^2 + \left(1 - \frac{2GM_{NS}}{c^2 r}\right)^{-1} dr^2 + r^2 (d\theta^2 + sen^2\theta d\phi^2)$$

- Geodesic equation:

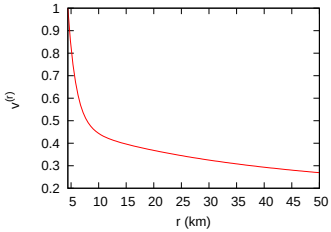

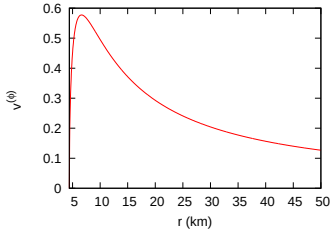

- Velocity modulus $v = \sqrt{\frac{2GM_{NS}}{r}}$, to $r = 12$ km $v \simeq 0.6c >> v_0 \simeq 200$ km/s
- The Lorentz factor: $\gamma(v) = \frac{1}{\sqrt{1-\frac{v^2}{c^2}}} \simeq 1.26 \Rightarrow |\vec{p}_\chi| c = \sqrt{\gamma^2 - 1} m_\chi c^2 \simeq 0.77 m_\chi c^2$
- De Broglie wavelength $\lambda = \frac{2\pi\hbar c}{|\vec{p}_\chi| c} \simeq \frac{2\pi 197.33\,\text{MeV fm}}{0.77 m_\chi c^2}$ puts a limit of validity m_χ few GeV

Dark matter particle-nucleon interaction

Medium effects in dark matter scattering
Introduction
GR boosted velocity
Cross-Section
Dark matter particle-nucleon interaction
Differential cross-section per unit volume
Cross-section and mean free path
Conclusions

$$\mathcal{L}_I = g_{Ns}\chi\bar{\chi}N\bar{N} + g_{Nv}\chi\gamma^\mu\bar{\chi}N\gamma_\mu\bar{N}$$

$p = (E, \vec{p})$, $p' = (E', \vec{p'})$
$k = (\omega, \vec{k})$, $k' = (\omega', \vec{k'})$
$q = p' - p = k - k'$
$q_0 = E' - E = \omega - \omega'$

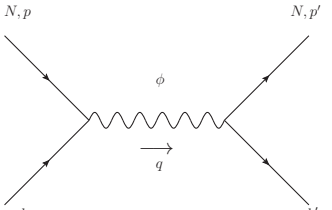

taking $q^2 << M_\phi^2 \Rightarrow$ point-like interaction
$g_{Ns} = g_{Nv} = G_F = 1.166\ 10^{-5}\ \mathrm{GeV}^{-2}$
$g_N \Rightarrow g_N F(|\vec{q}|^2)$

$F(|\vec{q}|^2) = \frac{\Lambda^2}{\Lambda^2 + q^2}$ monopolar form factor with
$\Lambda = 1.5\ \mathrm{GeV}$

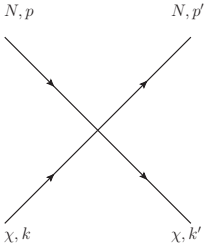

Dark matter particle-nucleon interaction

Medium effects in dark matter scattering
Introduction
GR boosted velocity
Cross-Section
Dark matter particle-nucleon interaction
Differential cross-section per unit volume
Cross-section and mean free path
Conclusions

The relativistic diferential cross-section:

$$d\sigma = \frac{|\overline{\mathcal{M}_N}|^2}{4\sqrt{(pk)^2 - m_N^{*2} m_\chi^2}} f_N(E)(1 - f_N(E'))(2\pi)^4 \delta^{(4)}(p + k - p' - k') \frac{d^3\vec{p'}}{(2\pi)^3 2E'} \frac{d^3\vec{k'}}{(2\pi)^3 2\omega'}$$

$f_N(E) = \frac{1}{1+e^{\frac{E-\mu_N^*}{T}}}$ Fermi-Dirac distribution functions, where $T(MeV)$ temperature of the star, μ_N^* effective nucleon chemical potential

- For the dark sector we assume $f_\chi(\omega') \approx 0$, all outgoing states allowed
- If we consider a finite temperature we must take into account the detailed balance factor

$$S(q_0, T) = \frac{1}{1 - e^{-\frac{|q_0|}{T}}}$$

- $|\overline{\mathcal{M}}_N|^2 \simeq 4g_{Ns}^2(E'E + m_N^{*2})(\omega'\omega + m_\chi^2) + 8g_{Nv}^2(2m_N^{*2}m_\chi^2 - m_N^{*2}\omega\omega' - m_\chi^2 E'E + 2E'\omega' E\omega)$ $+8g_{Ns}g_{Nv}m_N^* m_\chi(E + E')(\omega + \omega')$ and $\sqrt{(pk)^2 - m_N^{*2}m_\chi^2} \simeq \sqrt{E^2\omega^2 - m_N^{*2}m_\chi^2}$ at lowest order in velocities
- Medium effects parametrized in effective mass $m_N^*/m_N = 0.4, 0.7, 0.85$ for $n/n_{sat} = 2, 1, 0.5$

Differential cross-section per unit volume

Medium effects in dark matter scattering
Introduction
GR boosted velocity
Cross-Section
Dark matter particle-nucleon interaction
Differential cross-section per unit volume
Cross-section and mean free path
Conclusions

$$\frac{1}{V}\frac{d\sigma}{d\Omega dq_0} = \int_{|\vec{p}_-|}^{\infty} \frac{d|\vec{p}||\vec{p}|}{4(2\pi)^4 E'} \frac{m_N^* |\vec{k'}|}{|\vec{q}|} \delta(cos\ \theta - cos\ \theta_0)\Theta(|\vec{p}|^2 - |\vec{p}_-|^2) \frac{|\overline{\mathcal{M}}_{\mathcal{N}}|^2 f_N(E)(1-f_N(E'))S(q_0,T)}{4\sqrt{E^2\omega^2 - m_N^{*2} m_\chi^2}}$$

$$-\infty < q_0 \leqslant \omega - m_\chi$$

Kinematical restrictions:

- $T \sim 10^{-2}\,\mathrm{MeV}$ (evolved and cold star), $T << K_F = E_F - m_N^* \Rightarrow T \simeq 0$

$$0 \leqslant q_0 \leqslant \omega - m_\chi \quad \text{and} \quad \mathrm{S(q_0, T) = 1}$$

- $cos\ \theta_0 = \frac{m_N^*}{|\vec{p}||\vec{q}|}\left(q_0 - \frac{|\vec{q}|^2}{2m_N^*}\right)$ and $|cos\ \theta_0| \leqslant 1 \Rightarrow$

$$\frac{|\vec{q}|}{2m_N^*}(|\vec{q}| - 2|\vec{p_F}|) \leqslant q_0 \leqslant \frac{|\vec{q}|}{2m_N^*}(|\vec{q}| + 2|\vec{p_F}|)$$

$|\vec{p_F}| \equiv$ Fermi nucleon momentum

Results: Differential cross-section per unit volume

Medium effects in dark matter scattering
Introduction
GR boosted velocity
Cross-Section
Dark matter particle-nucleon interaction
Differential cross-section per unit volume
Cross-section and mean free path
Conclusions

arXiv: 1511.04071

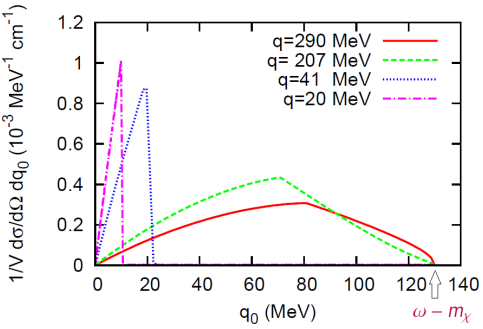

With $m_\chi = 500$ MeV, $n = n_{sat}$, $T = 0$

Results: Differential cross-section per unit volume

Medium effects in dark matter scattering
Introduction
GR boosted velocity
Cross-Section
Dark matter particle-nucleon interaction
Differential cross-section per unit volume
Cross-section and mean free path
Conclusions

$T \sim 10^{-2}\,\mathrm{MeV}$ evolved and cold star, $T << K_F = E_F - m_N^* \Rightarrow T \simeq 0$
$T \propto (10 - 30)\,\mathrm{MeV}$ some minutes after the Supernova explosion

arXiv: 1511.04071

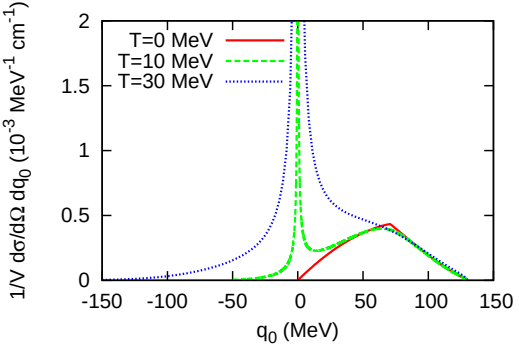

T (MeV)	n (fm^{-3})
0	0.17
10	0.174
30	0.209

$\mu = E_F$, $q = 207$ MeV and $m_\chi = 500$ MeV

Results: Mean free path

Medium effects in dark matter scattering
Introduction
GR boosted velocity
Cross-Section
Dark matter particle-nucleon interaction
Differential cross-section per unit volume
Cross-section and mean free path
Conclusions

Integrating over all possible outgoing energy values and solid angle we obtain the total integrated cross section per unit volume $\frac{\sigma(\omega)}{V}$ and the inverse of it, e.g. $\lambda_\chi^{-1} = \frac{\sigma(\omega)}{V}$ mean free path

$$\lambda_\chi^{-1} = \frac{\sigma(\omega)}{V} = \frac{m_N^*}{4(2\pi)^3}\int_0^{\omega - m_\chi} dq_0 \int_{|\vec{k}|-|\vec{k'}|}^{|\vec{k}|+|\vec{k'}|} d|\vec{q}| \int_{|\vec{p}_-|}^{\infty} d|\vec{p}| \frac{|\overline{\mathcal{M}}_N|^2 |\vec{p}| f_N(E)(1 - f_N(E'))}{4E'|\vec{k}|\sqrt{E^2\omega^2 - m_N^{*2} m_\chi^2}}$$

arXiv: 1511.04071

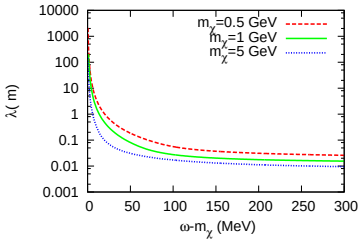

$n = n_{sat}$ and $T = 0$

$\lambda << R_{NS} \Rightarrow$ Diffusive scattering

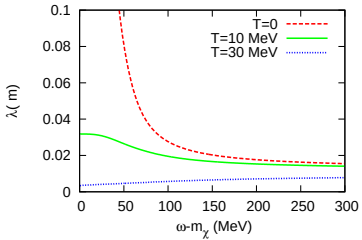

$\mu = E_F$, $m_\chi = 1$ GeV, $n(T = 0) = n_{sat}$,
$n(T = 10\ \text{MeV}) = 0.174\ \text{fm}^{-3}$ and $n(T = 30\ \text{MeV}) = 0.209\ \text{MeV}$

Results: Mean free path

Medium effects in dark matter scattering
Introduction
GR boosted velocity
Cross-Section
Dark matter particle-nucleon interaction
Differential cross-section per unit volume
Cross-section and mean free path
Conclusions

arXiv: 1511.04071

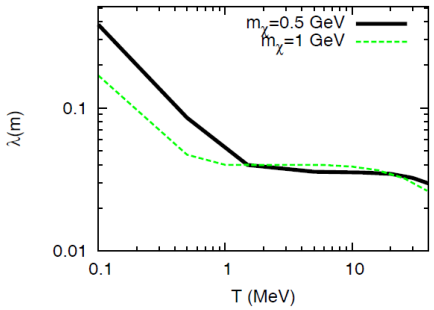

$n = 2n_{sat}$ and $\omega = 1.26$ GeV

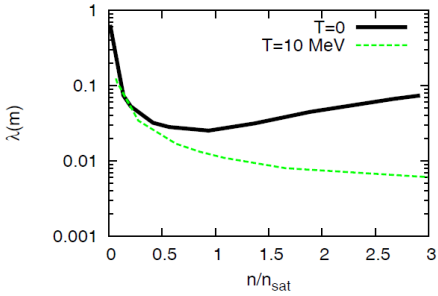

$m_\chi = 1$ GeV and $\omega = 1.26$ GeV

$\lambda << R_{NS} \Rightarrow$ Diffusive scattering

Is the cross section obtained consistent with collider current constraints?

Medium effects in dark matter scattering
Introduction
GR boosted velocity
Cross-Section
Dark matter particle-nucleon interaction
Differential cross-section per unit volume
Cross-section and mean free path
Conclusions

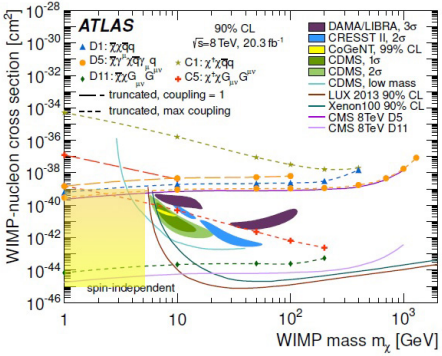

M. Klasen, M. Pohl, and G. Sigl,
Prog. Part. Nucl. Phys. 85 (2015) 1–32

If we consider $n = 2n_{sat}$ we can estimate $\sigma \sim \frac{\sigma/V}{n}$ for $\sqrt{s} \lesssim 6\ \mathrm{GeV}$ to compare to EFT analysis.
The values we obtain for scalar and vector couplings range $\sigma \sim 10^{-39} - 10^{-40}\ \mathrm{cm}^2$ and they are consistent with collider constraints considering weak couplings

Considering the best upper limits given by ATLAS and CMS and taking into account the lower limit given by the geometrical cross-section, $\sigma \gtrsim \sigma_0 \sim 10^{-45}\ \mathrm{cm}^2$, we obtain:

$$10^{-3} G_F \lesssim g_{Ns} \lesssim 10 G_F$$

$$10^{-3} G_F \lesssim g_{Nv} \lesssim G_F$$

Conclusions

Medium effects in dark matter scattering
Introduction
GR boosted velocity
Cross-Section
Dark matter particle-nucleon interaction
Differential cross-section per unit volume
Cross-section and mean free path
Conclusions

- We have calculated the interaction cross-section taking the medium into consideration.
- Inside the core mean free path $\lambda << R_{NS} \Rightarrow$ diffusive scattering .
- Peak effects seen on the differential cross section are due to Fermi step function at $T \sim 0$.
- At finite T states with negative tranferred energies are considered and because of the detailed balance factor a divergence close $q_0 = 0$ appears.
- The mean free path decreases with larger masses and larger kinetic energies at $T \sim 0$.
- λ decreases when T increases being a larger effect at lower kinetic energies.
- The behavior of λ both with $\omega - m_\chi$ and n changes with T.
- λ is monotically increasing with n but this is reversed for $T \sim 0$.
- The values of σ/V are consistent with collider current constraints considering weak couplings and we could set limits for g_{Ns} and g_{Nv}.

VILA DO CONDE,
PORTUGAL,
29-31 MARCH, 2016

11th Iberian Cosmology Meeting

IBERICOS 2016

SERIES OF MEETINGS WHICH AIM TO ENCOURAGE INTERACTIONS AND COLLABORATIONS BETWEEN RESEARCHERS WORKING IN COSMOLOGY AND RELATED AREAS IN PORTUGAL AND SPAIN.

www.iastro.pt/ibericos2016

ia instituto de astrofísica e ciências do espaço

FCT Fundação para a Ciência e a Tecnologia

U.PORTO

Vila do Conde

TEATRO MUNICIPAL VILA DO CONDE

THE CHAPLYGIN GAS IN THE MECHANICAL APPROACH

João Morais (UPV/EHU)

IberiCOS XI (2016)

Based on the work:

M. Bouhmadi-López et al., *JCAP 12 (2015) 037*
arXiv:1509.06963 [gr-qc]

eman ta zabal zazu
Universidad del País Vasco
Euskal Herriko Unibertsitatea

ZTF-FCT
Zientzia eta Teknologia Fakultatea
Facultad de Ciencia y Tecnología

MODIFIED GENERALISED CHAPLYGIN GAS (mGCG)

The mGCG is a barotropic fluid with the equation of state (cf. **[Benaoum2002]**)

$$\bar{p}_{\mathrm{Ch}} = \beta\bar{\varepsilon}_{Ch} - (1+\beta)\frac{A}{\bar{\varepsilon}^{\alpha}_{Ch}}$$

$$\beta \neq -1 \qquad\qquad \alpha \neq -1$$

The Chaplygin gas ($\beta = 0,\ \alpha = 1$) was introduced in **[Kamenshchik2001]** as a way to explain the current acceleration.

Generalisations of the Chaplygin gas, **[Bento2002]** ($\beta = 0$) and **[Benaoum2002]**, were developed shortly after.

Initial interest due to the possibility of unification of the dark sector but instabilities were detected at the perturbative level **[Bento2004]**

Applications in early universe cosmology, **[Bouhmadi-López2010]**, and treatment of singularities, **[Bouhmadi-López2005]**.

MODIFIED GENERALISED CHAPLYGIN GAS (mGCG)

In a FLRW universe:

$$\frac{\bar{\varepsilon}_{\mathrm{Ch}}}{\bar{\varepsilon}_{\mathrm{Ch},0}} = \left[A_s + (1 - A_s)\left(\frac{a_0}{a}\right)^{3\xi}\right]^{\frac{1}{1+\alpha}}$$

$$\xi := (1+\alpha)(1+\beta) \qquad A_s := A/\bar{\varepsilon}^{1+\alpha}$$

The mGCG can behave as a fluid with EoS parameter $w \sim \beta$ and as an effective cosmological constant.

Reparametrizing:

$$\frac{\bar{\varepsilon}_{\mathrm{Ch}}}{\bar{\varepsilon}_{\mathrm{Ch},*}} = \left[\mathrm{sgn}(A_s) + \mathrm{sgn}(1 - A_s)\left(\frac{a_*}{a}\right)^{3\xi}\right]^{\frac{1}{1+\alpha}}$$

$$a_* := a_0 \left|\frac{1 - A_s}{A_s}\right|^{\frac{1}{3\xi}} \qquad \bar{\varepsilon}_{\mathrm{Ch},*} := |A|^{\frac{1}{1+\alpha}}$$

The value a_* marks the transition moment between the two behaviours.

MODIFIED GENERALISED CHAPLYGIN GAS (mGCG)

The qualitative behaviour of the mGCG depends on the parameters of the model:

- $\xi > 0$ or $\xi < 0$
- $A_s < 0$, $0 < A_s < 1$, or $1 < A_s$
- $\alpha > -1$ (full) or $\alpha < -1$ (dashed)

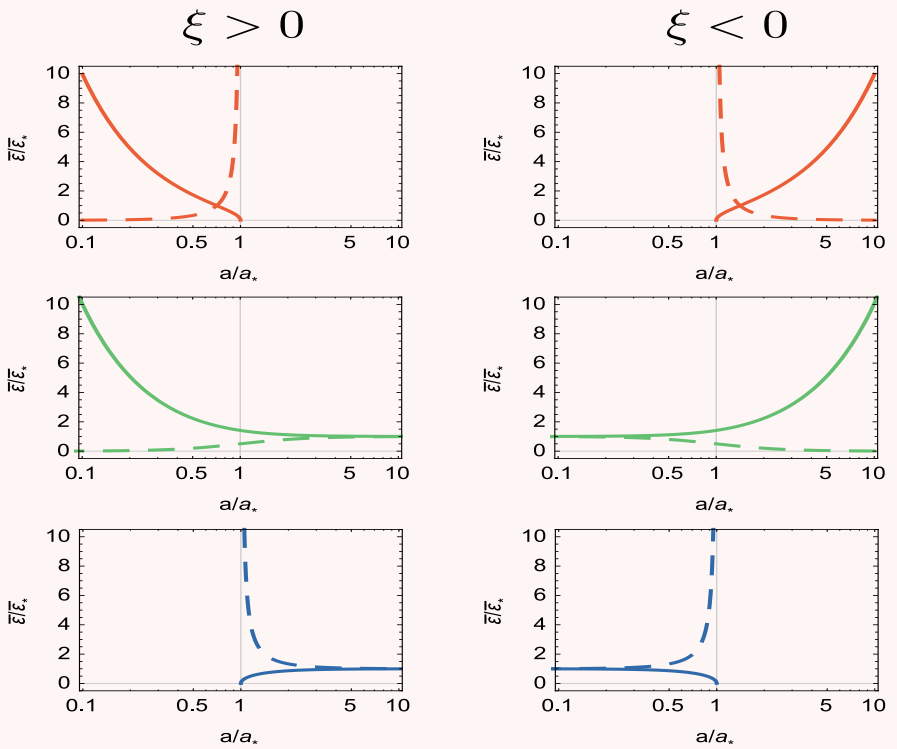

MECHANICAL APPROACH

A new method, developed in [Eingorn2012], [Eingorn2013], and [Eingorn2014], based on the discrete cosmology to study the late-time evolution of the Universe.

- The universe is considered well inside the cell of uniformity $l <\sim 150$ Mpc.
- The Large Scale Structure of the Universe is assumed to have already formed $z <\sim 10$.

- Galaxies and groups of galaxies are treated as point-like structures with non-relativistic peculiar velocities.
- Appropriate to study the dynamics of astrophysical bodies on the cosmological background [Eingorn2013].
- Predicts the presence of the Hubble Flow at distances smaller than 3 Mpc from the center of our group of galaxies [Eingorn2012].

MECHANICAL APPROACH
BACKGROUND

Dynamics dictated by

Friedmann Eq:

$$\frac{3\left(\mathcal{H}^2+\mathcal{K}\right)}{a^2}=\kappa^2\left(\bar{T}_0^0+\bar{\varepsilon}_{\mathrm{rad}}+\bar{\varepsilon}_{\mathrm{de}}\right)$$

Raychaudhury Eq:

$$\frac{2\mathcal{H}'+\mathcal{H}^2+\mathcal{K}}{a^2}=-\kappa^2\left(\frac{1}{3}\bar{T}_i^i+\bar{p}_{\mathrm{rad}}+\bar{p}_{\mathrm{de}}\right)$$

For a collection of p point-like bodies of masses m_p [Eingorn2012]

$$T^{\mu\nu}=\sum_p \frac{m_p c^2}{\sqrt{-g}}\frac{dx^\mu}{ds}\frac{dx^\nu}{ds}\frac{ds}{d\eta}\delta(\mathbf{r}-\mathbf{r_p})$$

At the background level the only non-zero component is

$$\bar{T}_0^0=\frac{\bar{\rho}_c c^2}{a^3} \qquad \bar{\rho}_c:=\frac{1}{\sqrt{\gamma}}\sum_p m_p\delta(\mathbf{r}-\mathbf{r_p})$$

γ – determinant of the spatial metric.

MECHANICAL APPROACH
PERTURBATIONS

In the case of non-relativistic velocities (cf. [Eingorn2012])

$$\Phi = \frac{\varphi c^2}{a}$$

$$\delta T_0^0 = \frac{\delta \rho_c c^2}{a^3} + \frac{3\bar{\rho}_c c^2 \varphi}{a^4}$$

$$\delta T_i^i = 0$$

Accuracy of the method fixed at $O(a^{-4})$ (cf. [Akarsu2015])

$$\delta\varepsilon_{\mathrm{rad}} \sim \frac{1}{a^4}$$

Assuming a contribution from dark energy

$$\delta\varepsilon_{\mathrm{rad}} = -\frac{3\bar{\rho}_c \varphi}{a^4} + \delta\varepsilon_{\mathrm{rad},2}$$

MECHANICAL APPROACH
PERTURBATIONS

The master equations become

$$-\left(\bar{\varepsilon}_{\mathrm{de}}+\bar{p}_{\mathrm{de}}\right)\frac{\varphi}{c^2 a}=\delta p_{\mathrm{de}}+\frac{1}{3}\delta\varepsilon_{\mathrm{rad},2}$$

$$\Delta\varphi+3\mathcal{K}\varphi-\frac{\kappa^2 c^4}{\delta\rho_c}=\frac{\kappa^2 c^2 a^3}{2}\delta\varepsilon_{\mathrm{de}}+\frac{\kappa^2 c^2 a^3}{2}\delta\varepsilon_{\mathrm{rad},2}$$

The left-hand-side of the second master equation is independent of time.

In the case of barotropic fluis the first master equation gives

$$\delta\varepsilon_{\mathrm{de}}(\varphi,\delta\varepsilon_{\mathrm{rad},2})$$

Substitution on the second master equation must lead to a right-hand-side that is time-independent!

Non-vanishing right-hand-side leads to the screening of the gravitational potential.

MECHANICAL APPROACH
THE CASE OF THE mGCG

The mGCG is a barotropic fluid with

$$\delta p_{\rm Ch} = \frac{A_s(\xi-1)+(1-A_s)\beta(\frac{a_0}{a})^{3\xi}}{A_s+(1-A_s)(\frac{a_0}{a})^{3\xi}}\delta\varepsilon_{\rm Ch}$$

In [Bouhmadi-López2015] we consider mGCG with $0 < A_s < 1$ and search the parameter space (ξ,β) for the models compatible with the Mechanical Approach.

From the first master equation we obtain

$$\delta\varepsilon_{\rm Ch} = -\left[A_s+(1-A_s)\left(\frac{a_0}{a}\right)^{3\xi}\right]^{\frac{1}{1+\alpha}} \frac{(1-A_s)(1+\beta)(\frac{a_0}{a})^{3\xi}}{A_s(\xi-1)+(1-A_s)\beta(\frac{a_0}{a})^{3\xi}}\frac{\bar{\varepsilon}_{\rm de}}{c^2 a}\varphi$$

$$-\frac{1}{3}\frac{A_s+(1-A_s)\left(\frac{a_0}{a}\right)^{3\xi}}{A_s(\xi-1)+(1-A_s)\beta\left(\frac{a_0}{a}\right)^{3\xi}}\delta\varepsilon_{\rm rad2}$$

MECHANICAL APPROACH
mGCG (RESULTS)

ξ	$\delta\varepsilon_{\mathrm{rad},2}$	$\delta\varepsilon_{\mathrm{Ch}}$	late-time	screening
$\xi > 0,\ \xi \neq 4/3$	0	0	cosmo. constant	no
$\xi = 4/3$	can be non-zero	$\propto \delta\varepsilon_{\mathrm{rad},2}$	cosmo. constant	no
$\xi = 2/3$	0	non-zero	cosmo. constant	yes
$\xi < 0,\ \beta > 0,\ \beta \neq 1/3$	0	0	deceleration	no
$\xi < 0,\ \beta = 1/3$	can be non-zero	$\propto \delta\varepsilon_{\mathrm{rad},2}$	deceleration	no
$\xi < -1/3,\ \beta = -1/3$	0	non-zero	zero-acceleration	yes

MECHANICAL APPROACH mGCG (RESULTS)

- We have studied the compatibility of the mGCG models playing the role of dark energy with the Mechanical Approch .
- We found mGCG compatible with the Mechanical Approach that lead to late-time acceleration.
- Although compatible with the approach, the physical feasability of these solutions is unclear.

- In the cases compatible with observations there is no clustering of the mGCG

$\xi \in [0.8492, 1.4588]$ **[Lu2011]**

$\xi \in [0.795, 2.032]$ **[Sharov2015]**

- The case with $\xi = 2/3$ leads to clustering of the mGCG but is outside the observational constraints.

VILA DO CONDE,
PORTUGAL,
29-31 MARCH, 2016

11th Iberian Cosmology Meeting

IBERICOS 2016

SERIES OF MEETINGS WHICH AIM TO ENCOURAGE INTERACTIONS AND COLLABORATIONS BETWEEN RESEARCHERS WORKING IN COSMOLOGY AND RELATED AREAS IN PORTUGAL AND SPAIN.

www.iastro.pt/ibericos2016

ia instituto de astrofísica e ciências do espaço

FCT Fundação para a Ciência e a Tecnologia

U.PORTO

Vila do Conde

TEATRO MUNICIPAL VILA DO CONDE

Nonlinear Chaplygin Gas Cosmologies

Vasco Ferreira

Ibericos 2016

Instituto de Astrofísica, Faculdade de Ciências da Universidade do Porto

30th March 2016

ΛCDM model

Universe is homogeneous and isotropic on large scales

$$ds^2 = g_{\mu\nu}dx^\mu dx^\nu = -dt^2 + a^2(t)\left[\frac{dr^2}{1-Kr^2} + r^2\left(d\theta^2 + sin^2\theta d\phi^2\right)\right]$$

GR provides an accurate description of gravity on cosmological scales

$$S_{E.H.} = \int d^4x\sqrt{-g}\left(\mathcal{L}_G + \mathcal{L}_M\right) \rightarrow G_{\mu\nu} = R_{\mu\nu} - \frac{1}{2}g_{\mu\nu}R = 8\pi G T_{\mu\nu}$$

$$\text{Continuity equation:} \quad \frac{d\rho}{dt} + 3H(\rho + p) = 0$$

$$\text{Perfect fluid: } T_{\mu\nu} = (\rho + p)u_\mu u_\nu + pg_{\mu\nu} \rightarrow \begin{cases} p_{CDM} = 0 \rightarrow \rho_{CDM} \propto a^{-3} \\ p_\Lambda = -\rho_\Lambda \rightarrow \rho_\Lambda \propto const. \end{cases}$$

$$\text{Late universe:} \quad H^2 = \frac{8\pi G}{3}\left[\rho_b + \rho_{CDM} + \rho_\Lambda\right]$$

Generalized Chaplygin Gas

Introduction

Perfect fluid and baratropic equation of state [1,2]

$$p_{cg} = -\frac{A}{\rho_{cg}^{\alpha}} \qquad , \qquad 0 \leqslant \alpha \leqslant 1$$

From the continuity equation

$$\rho_{cg} = \rho_{cg}^{(0)} \left[\overline{A} + \left(1 - \overline{A} \right) a^{-3(1+\alpha)} \right]$$

- $a \ll 1 \qquad \rho_{cg} \propto \left(1 - \overline{A} \right)^{\frac{1}{1+\alpha}} a^{-3}$
- $a \gg 1 \qquad \rho_{cg} \propto \overline{A}^{\frac{1}{1+\alpha}}$

EoS parameter: $w_{cg} = \frac{p_{cg}}{\rho_{cg}} = -\frac{A}{\rho_{cg}^{1+\alpha}}$

Sound speed: $c_s^2 = \frac{\partial p}{\partial \rho} = -\alpha w_{cg}$

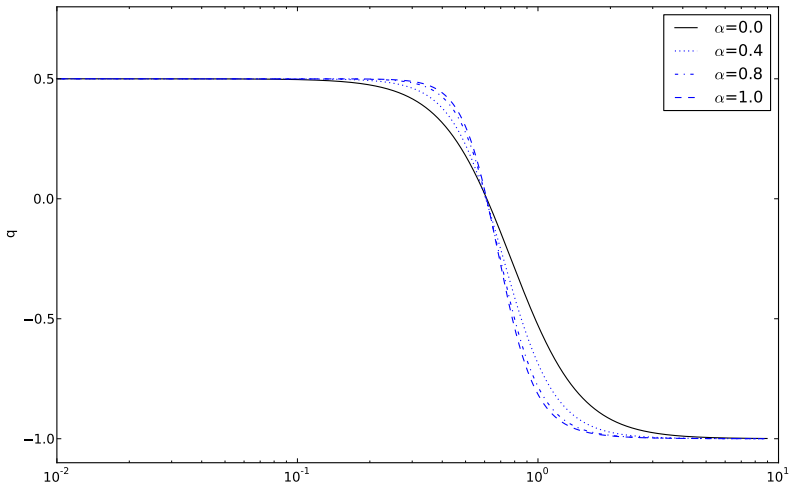

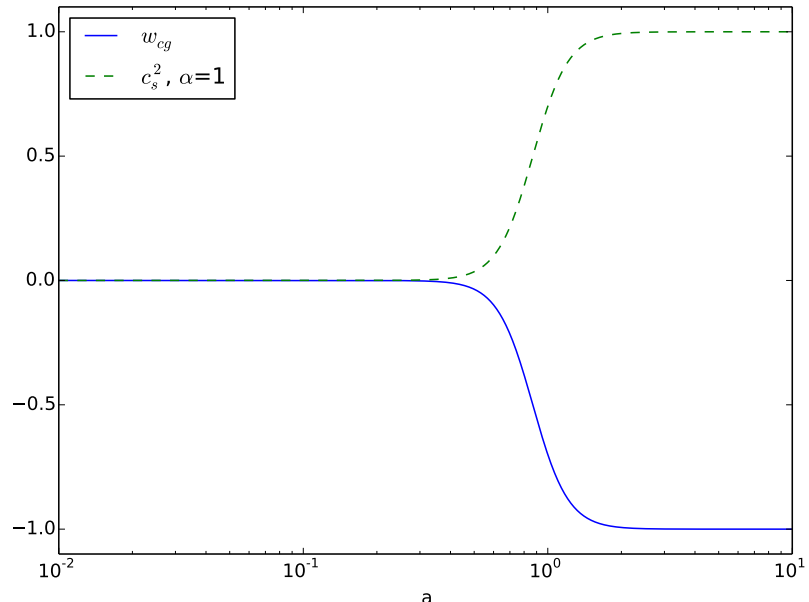

[1] A.Y. Kamenshchik et al, Phys. Lett. B 511, 265 (2001)

Bento M.C. et al, Phys. Rev. D, 66, 043507 (2002)

Generalized Chaplygin Gas

Observational Constraints

Background

Restricts $\alpha \lesssim 0.4$ and $0.69 \lesssim \overline{A} \lesssim 0.77$

Linear regime

Matter power spectrum: $0 \leqslant \alpha \leqslant 1$
(considering baryons)
CMB (late ISW): $\alpha \sim 0$

- GCG with $\alpha = 0$ is equivalent to ΛCDM model at all orders.[3]
- By gravitation alone we can not distinguish between both models.

[3] P.P. Avelino et al, Phys.Rev. D77 (2008) 063515

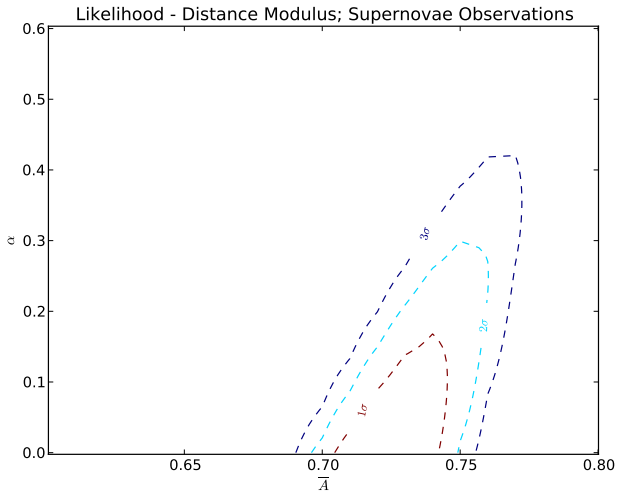

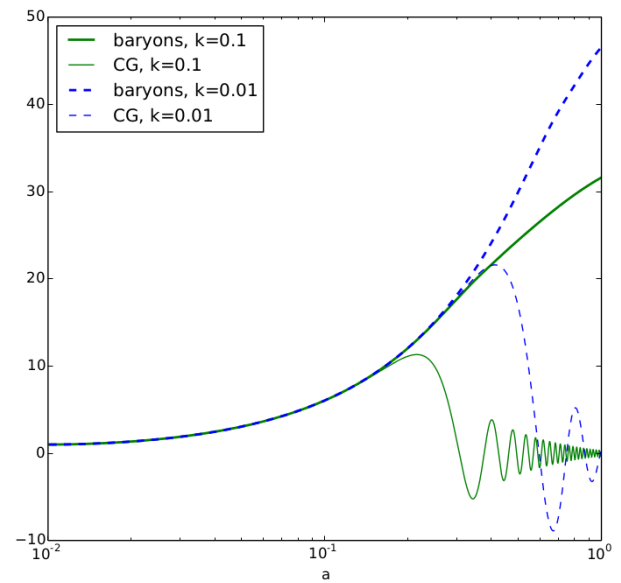

Generalized Chaplygin Gas

Small Scales

Mass Dispersion: $\sigma(R, a)$

- Early on, both fluids evolve in the same way on all relevant scales
- Later, the pressure p_{cg} increases so $c_{cg,s} \neq 0$ prevents the further collapse of the CG

However, on small scales a significant fraction of the CG will have collapsed and decoupled from the background. [4]

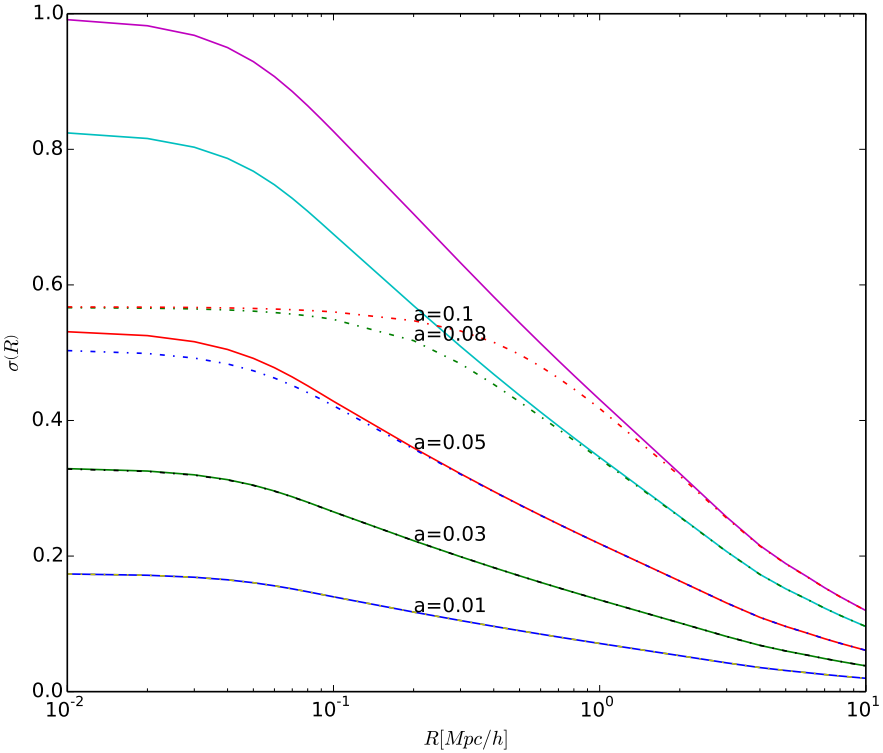

[4] P.P. Avelino et al. The onset of the nonlinear regime in unified dark matter models. Phys. Rev. D68 (2004), 041301

Nonlinear Chaplygin Gas

Introduction

- Collapsed regions: $\rho_+ \gg \langle \rho_{cg} \rangle$
- Underdense regions: $\rho_- \ll \langle \rho_{cg} \rangle$
- Parameterization of small scale nonlinear clustering: $\epsilon = \frac{E_+}{E}$

$$\rho_+ = \epsilon \langle \rho_{cg} \rangle , \rho_- = (1-\epsilon) \langle \rho_{cg} \rangle$$

$$w_{cg} = \frac{p_-}{\langle \rho_{cg} \rangle} = (1-\epsilon) w_-$$

$$H^2 = \frac{8\pi G}{3} [\rho_b + \langle \rho_{cg} \rangle]$$

[5] P.P.Avelino, K.Bolejko and G.F.Lewis. Nonlinear Chaplygin gas cosmologies. Phys. Rev.,D89:103004, 2014

Nonlinear Chaplygin Gas

Background evolution

ϵ_i: Initial fraction of small scale clustering

$$\epsilon_i = \frac{E_+}{\rho_i a^3} \to \text{const.}$$

We assume that E_+ remain constant

$$\boxed{\frac{a}{\langle \rho_{cg} \rangle} \frac{d\langle \rho_{cg} \rangle}{da} + 3(1 + w_{cg}) = 0}$$

$$w_{cg} = -(1-\epsilon) \frac{A}{\left[(1-\epsilon)\langle \rho_{cg} \rangle\right]^{1+\alpha}}$$

$$\boxed{w_- = -\frac{A}{\left[(1-\epsilon)\langle \rho_{cg} \rangle\right]^{1+\alpha}}}$$

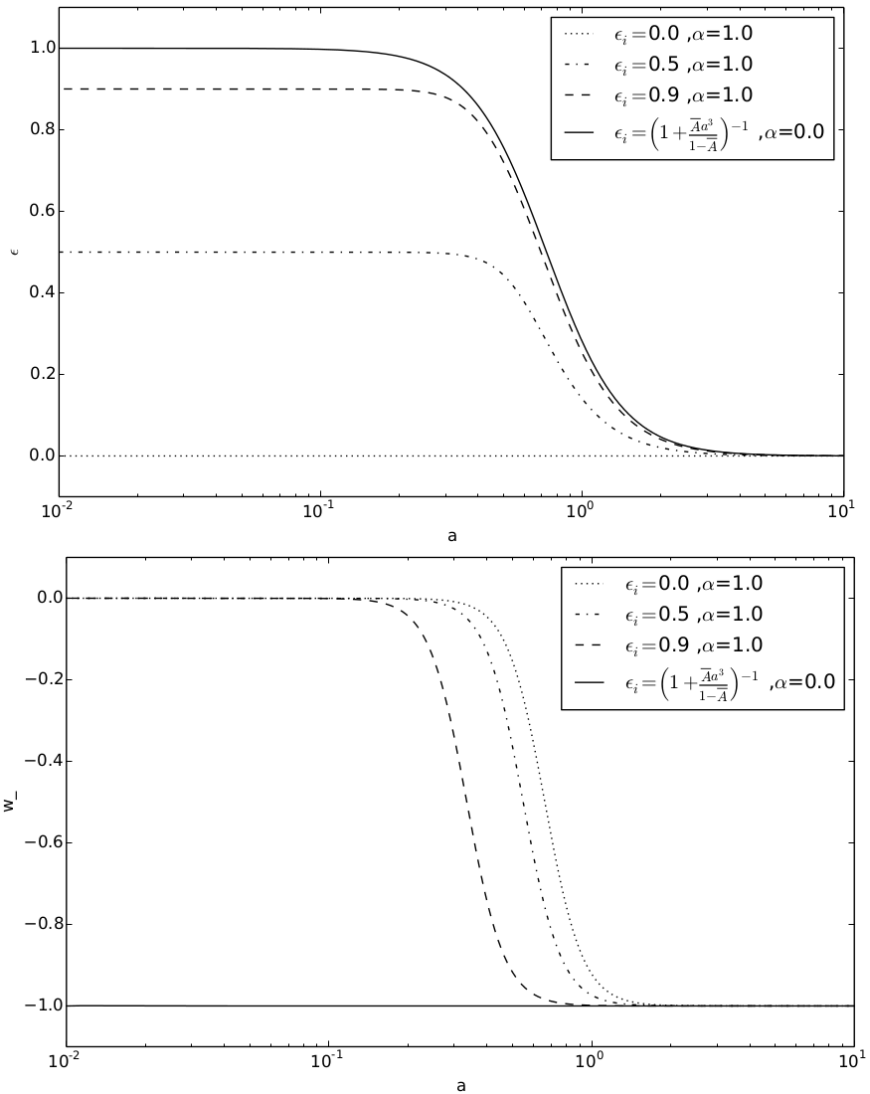

Nonlinear Chaplygin Gas

Obervational constraints

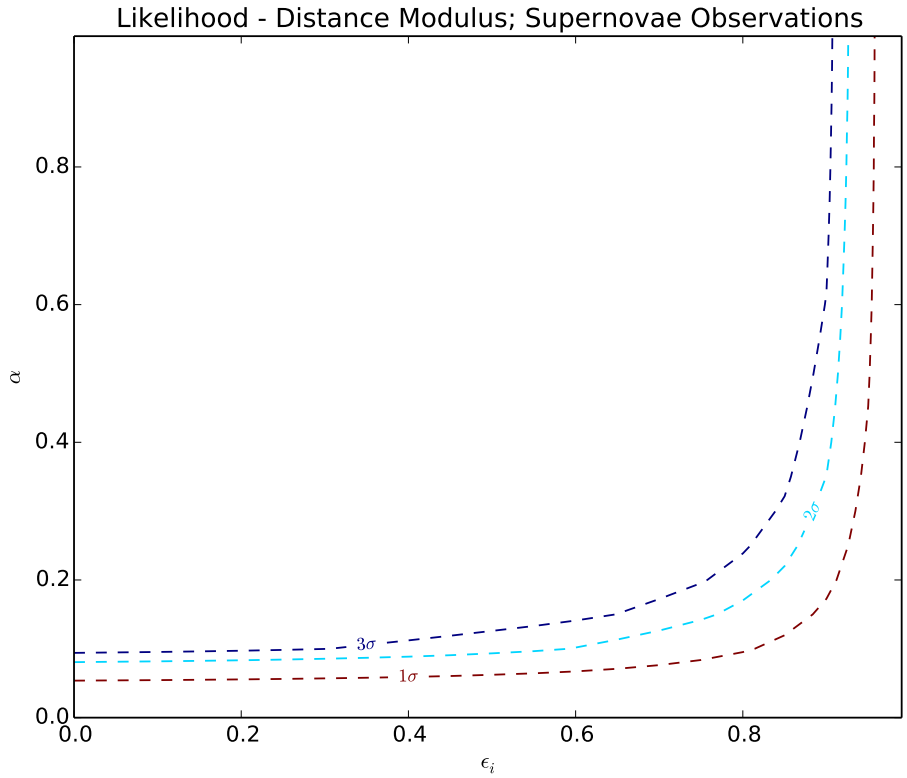

Confidence region for the Nonlinear CG parameters. All range of values for α are admissible if ϵ_i is high enough.

Nonlinear Chaplygin Gas

Density perturbations

- Collapsed regions: δ_+
- Underdense regions: δ_-
- $\Omega_+ = \epsilon$, $\Omega_- = 1 - \epsilon$

Perturbation equations

$$\begin{cases} \delta_+'' + (2+\xi)\,\delta_+' = \frac{3}{2}\left[\Omega_+\delta_+ + \left(1 - 3\alpha w_-\right)\Omega_-\delta_-\right] \\ \delta_-' + (1+w_-)\left(\frac{\theta_-}{\mathcal{H}} - \delta_+'\right) = 3w_-\,(1+\alpha)\,\delta_- \\ \theta_-' + \left(1+3\alpha w_-\right)\theta_- = -\frac{\alpha w_-\, k^2}{\mathcal{H}\left(1+w_-\right)}\delta_- \end{cases}$$

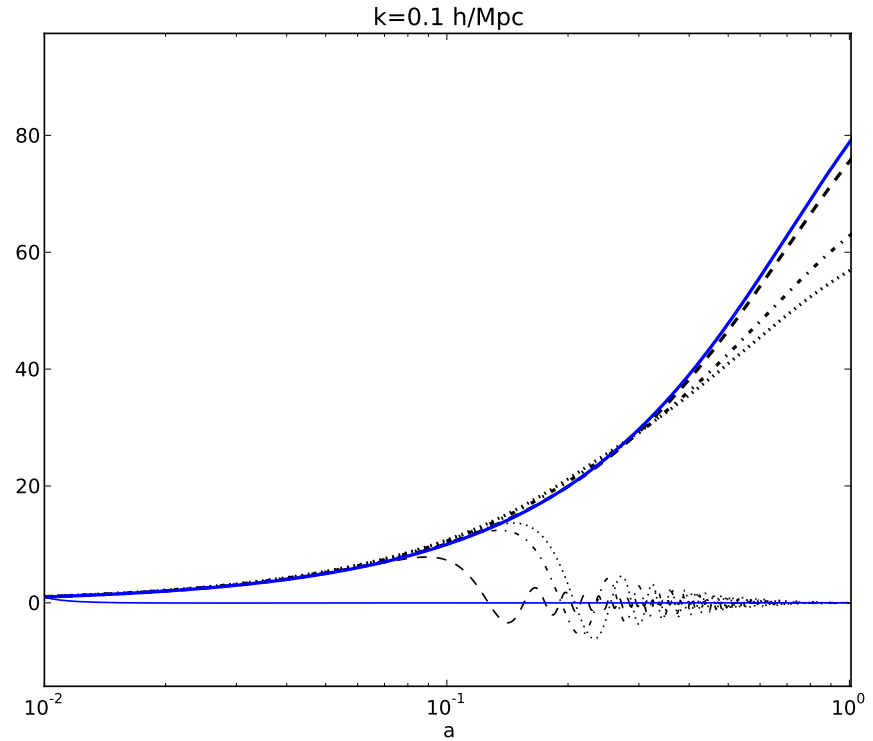

Nonlinear Chaplygin Gas

Matter Power Spectrum

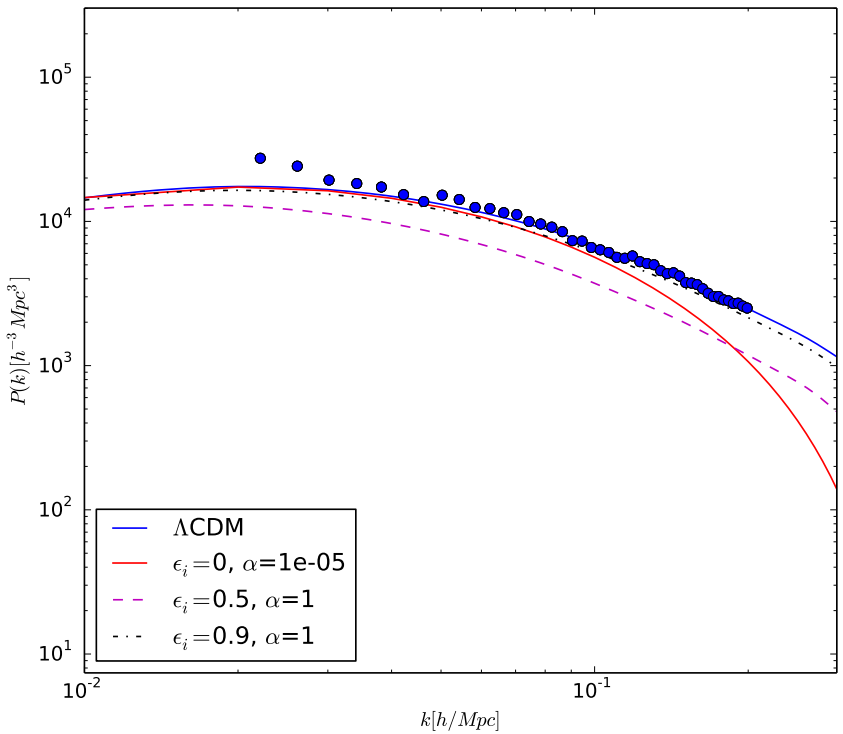

The matter power spectrum is consistent with the obervations for all range of values for α considering that ϵ_i is high enough.

Nonlinear Chaplygin Gas

Density perturbations - late ISW effect

Growth function

$$D(a) = \frac{\delta(a)}{\delta_i}$$

$\frac{D(a)}{a} \approx$ const. during the matter era.

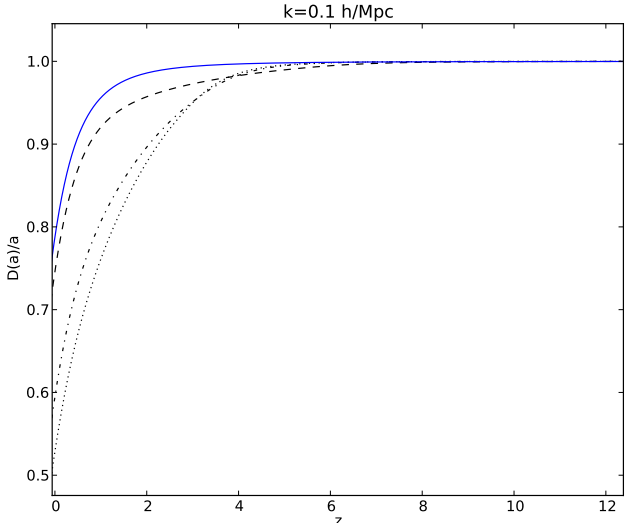

Late ISW effect

$$\Theta_l(k) = -2\int e^{\tau(z)}\frac{\partial\Phi}{\partial z} j_l[kr(z)]\,dz$$

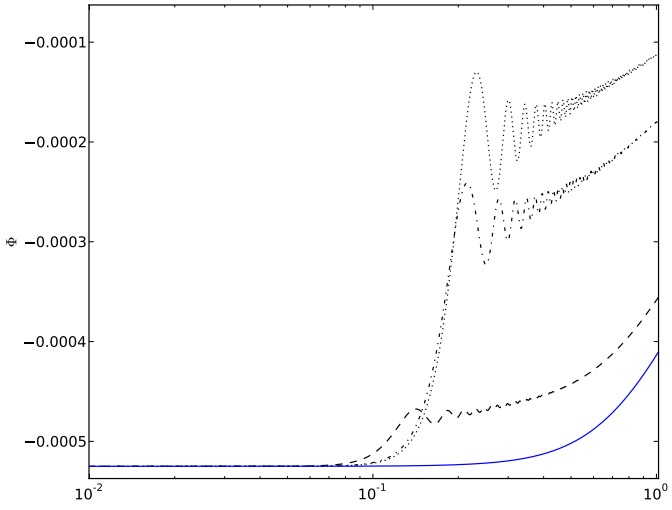

Summary

GCG

- Background dynamics:

$$\alpha \lesssim 0.4 \qquad , \qquad 0.69 \lesssim \overline{A} \lesssim 0.77$$

- Linear Perturbation Theory:
  - highly restricts the parameter space ($\alpha \lesssim 10^{-5}$)
  - although baryons play an important role on structure formation, the restriction is not significantly alleviated

Nonlinear Chaplygin Gas Cosmologies

- Nonlinear clustering on small scales should be taken in account (ϵ)
- Models with sufficiently high ϵ have a background dynamics and structure formation consistent with the observations for $0 \leq \alpha \leq 1$.

VILA DO CONDE,
PORTUGAL,
29-31 MARCH, 2016

11th Iberian Cosmology Meeting

IBERICOS 2016

SERIES OF MEETINGS WHICH AIM TO ENCOURAGE INTERACTIONS AND COLLABORATIONS BETWEEN RESEARCHERS WORKING IN COSMOLOGY AND RELATED AREAS IN PORTUGAL AND SPAIN.

www.iastro.pt/ibericos2016

ia instituto de astrofísica e ciências do espaço

FCT Fundação para a Ciência e a Tecnologia

U.PORTO

Vila do Conde

TEATRO MUNICIPAL VILA DO CONDE